



Agenzia Nazionale per le Nuove Tecnologie,  
l'Energia e lo Sviluppo Economico Sostenibile

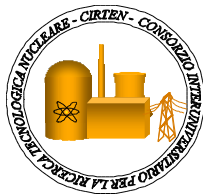


*Ministero dello Sviluppo Economico*

RICERCA DI SISTEMA ELETTRICO

# Benchmark on Thermo-Fluid Dynamics of an Open Square Lattice Core of a Lead Cooled Reactor with SIMMER-III and FEM-LCORE Codes

*G. Bandini, M. Polidori*



BENCHMARK ON THERMO-FLUID DYNAMICS OF FAN OPEN SQUARE LATTICE CORE OF A LEAD  
COOLED REACTOR WITH SIMMER-III AND FEM-LCORE CODES

G. Bandini ENEA, M. Polidori ENEA

Settembre 2010

Report Ricerca di Sistema Elettrico

Accordo di Programma Ministero dello Sviluppo Economico – ENEA

Area: Produzione e fonti energetiche

Tema: Nuovo Nucleare da Fissione

Responsabile Tema: Stefano Monti, ENEA

**Titolo**

**Benchmark on Thermo-Fluid Dynamics of an Open Square Lattice Core of a Lead Cooled Reactor with SIMMER-III and FEM-LCORE Codes**

**Descrittori**

**Tipologia del documento:** Rapporto Tecnico  
**Collocazione contrattuale:** Accordo di programma ENEA-MSE: tema di ricerca "Nuovo nucleare da fissione"  
**Argomenti trattati:** Generation IV reactors  
 Reattori nucleari veloci  
 Termoidraulica dei reattori nucleari

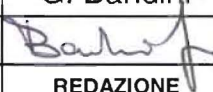
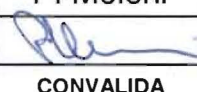
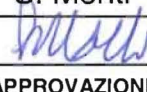
**Sommario**

This report deal with the validation of a thermo-fluid dynamic model for the lead-cooled reactor ELSY implemented on the finite element 3D FEM-LCORE code and developed by the DIENCA department of the University of Bologna. This model has been used for the investigation of pressure, velocity and temperature distributions inside the open square ELSY core. The main purpose of this work is to compare the FEM-LCORE results obtained by the University of Bologna with the results obtained by ENEA using a more validated code, under the same initial and boundary conditions. The 2D SIMMER-III code, which is widely used at international level for fast reactor thermo-fluid dynamic analysis, has been selected by ENEA for code to code result benchmarking. In spite of the less detailed 2D simulation of SIMMER-III code, a substantial agreement has been found with the FEM-LCORE results regarding pressure, velocity and temperature profiles over the whole core region.

**Note**

**Autori:**  
 G. Bandini, M. Polidori (UTFISSM-SICISIS)

**Copia n.**
**In carico a:**

2			NOME			
			FIRMA			
1			NOME			
			FIRMA			
0	EMMISSIONE	15.9.2010	NOME	G. Bandini	P. Meloni	S. Monti
			FIRMA			
REV.	DESCRIZIONE	DATA		REDAZIONE	CONVALIDA	APPROVAZIONE

## Table of Contents

1.	INTRODUCTION .....	3
2.	THE ELSY PLANT AND REACTOR CORE .....	4
	2.1 Core Geometry .....	4
	2.2 Core Power Distribution .....	6
3.	2D SIMMER-III SIMULATION.....	8
	3.1 The SIMMER-III Code .....	8
	3.2 SIMMER-III Model .....	8
	3.3 SIMMER-III Results .....	9
	3.3.1 Primary System Behaviour .....	9
	3.3.2 Reactor Core .....	11
4.	3D FEM-LCORE SIMULATION .....	18
	4.1 The FEM-LCORE Code .....	18
	4.2 FEM-LCORE Model .....	18
	4.3 FEM-LCORE Results .....	19
	4.3.1 Overall Calculation Domain .....	20
	4.3.2 Reactor Core .....	22
5.	SIMMER-III and FEM-LCORE RESULT COMPARISON .....	29
	5.1 Core Pressures .....	29
	5.2 Core Lead Velocities .....	30
	5.3 Core Lead Temperatures .....	32
	5.4 Influence of Upper Plenum FA Supporting Structures .....	33
6.	CONCLUSIONS .....	36
7.	REFERENCES .....	37
	Appendix A: SIMMER-III Input Deck .....	38

 <b>Ricerca Sistema Elettrico</b>	<b>Sigla di identificazione</b>	<b>Rev.</b>	<b>Distrib.</b>	<b>Pag.</b>	<b>di</b>
	NNFISS – LP3 - 001	0	L	3	58

## 1. INTRODUCTION

Within the framework of the previous national AdP ENEA-MSE program, the finite element FEM-LCORE code has been developed by the DIENCA department of the University of Bologna, in collaboration with ENEA, for thermo-fluid dynamic analysis of liquid metal reactors. The purpose of this code is to investigate three-dimensional pressure, velocity and temperature fields inside nuclear reactors at the coarse fuel assembly level. The solution of the Navier-Stokes system and the energy equation is obtained by using the finite element method. The numerical simulations take place at a coarse, assembly length level and are linked to the fine, sub-channel level state through transfer operators based on parametric coefficients that summarize local fluctuations. The overall effects between assembly flows are evaluated by using average assembly turbulent viscosity and energy exchange coefficients. The reactor upper and lower plenum region model is introduced by coupling the Navier-Stokes and energy system with a turbulence model.

Under the current AdP ENEA-MSE program, a thermo-fluid dynamic model for the lead-cooled reactor ELSY has been implemented on the 3D FEM-LCORE code by the University of Bologna. This model has been then applied to investigate the pressure, velocity and temperature distributions in different open/closed core configurations and in presence of control rods. Furthermore, a limited validation of the model has been carried out for the single fuel rod case on the basis of available experimental data. Consequently, a more extensive validation work on complex core geometries seems essential.

The main purpose of this work is the validation of the FEM-LCORE code by comparing the results obtained by the University of Bologna with the results obtained by ENEA using a more validated code, under the same core configuration and boundary conditions. The 2D SIMMER-III code, which is worldwide used for fast reactor thermo-fluid dynamic analysis, has been selected by ENEA for code to code result benchmarking. The open square design solution adopted for the ELSY core has been taken as reference core configuration. Indeed, in this case the turbulence inside the lower and upper plenum has significant effects on flow redistribution within the core, making the comparison more challenging and interesting from the point of view of turbulent code model validation.

## 42. THE ELSY PLANT AND REACTOR CORE

In the framework of the studies for the next generation of nuclear power plant well-known as GEN-IV, the ELSY (European Lead cooled System) project of the VI European Framework Program was addressed at the development of a European LFR (Lead Fast Reactor) design. The project aimed at investigating the technical/economical feasibility of a high power critical fast reactor with waste transmutation capability responding to the requirements of sustainability, non-proliferation and energy production at reasonable costs.

The ELSY plant [1] is a pool-type reactor of 1500 MWth cooled by lead with an electrical power of 600 MW. The scheme of the reactor block is shown in Fig. 1. The core power is removed by forced circulation of lead in the primary circuit through eight mechanical pumps, which are coaxial with the respective spiral tube steam generators and immersed in the annular and upper part of the lead pool. Inside the steam generators, the core heat is transferred to the secondary side by water vaporization at 180 bar pressure. The  $\Delta T$  through the core is of 80 °C, being the lead inlet temperature of 400 °C.

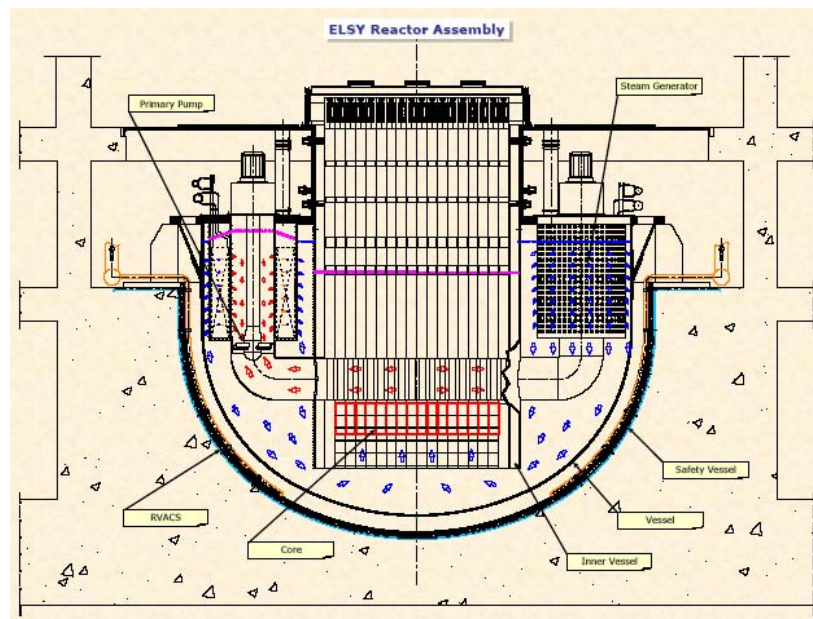


**Fig. 1 – Scheme of ELSY reactor block**

Such an innovative project needs the investigation of different design solutions that concern the overall power plant. The present study focuses the attention on the open square fuel assembly (FA) option adopted for the reactor core. The advantages to consider FAs without wrapper are quite evident, e.g. the in-vessel structures weight are reduced, there is less absorber material in the active core region, an increased power density, reduced risks of FA blockage, reduced hot-spot temperatures, etc.

### 2.1 Core Geometry

The ELSY reactor core consists of an array of 162 FAs wrapperless [2] with three different fuel enrichments in plutonium and 80 surrounding dummy/reflector assemblies. The reactor is

controlled by 8 scram control rods plus 70 finger absorbers sparse in the core for scram and regulation. A schematic view of ELSY core is shown in Fig. 2.

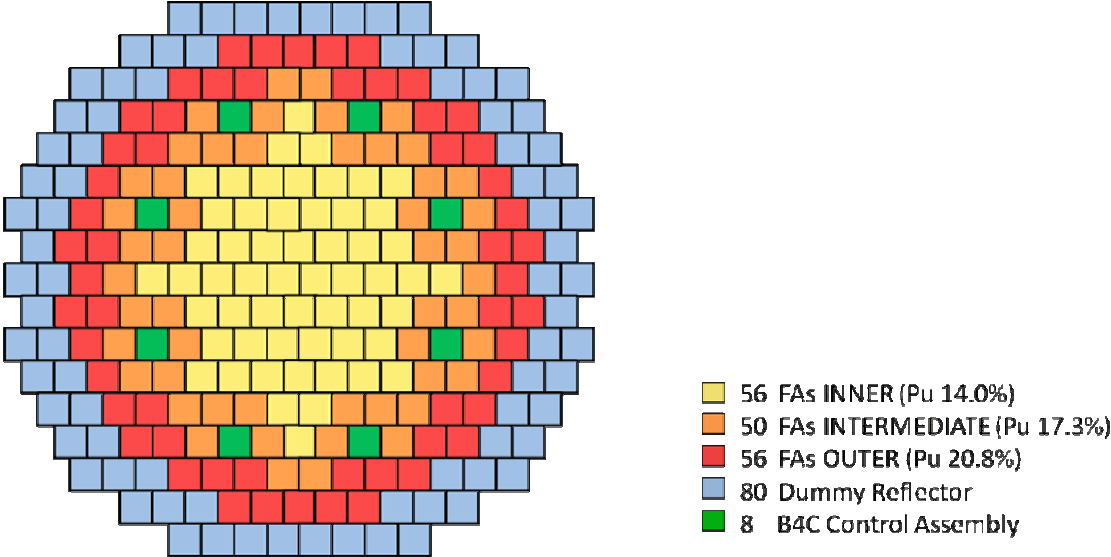


**Fig. 2 – Scheme of ELSY core**

The structure of the fuel assembly is characterized by a square lattice of 21 by 21 fuel pins of which the four angular ones are replaced with stainless steel structure for mechanical support. It is peculiar the presence of a structural void square tube located in the assembly centreline to host the finger absorber replacing 3 by 3 pins. The fuel pins are supported along their lengths with five spacer grids to maintain a constant distance among them. The fuel adopted is a MOX with three different plutonium enrichments (radially increasing) and the clad is made of ferritic-martensitic stainless steel T91. In particular, the fuel is hollowed to increase the volume for the gaseous fission products. This solution allows reaching a burnup of 100 MWd/kg, and reduces the maximum centreline fuel temperature. Fig. 3 shows the fuel assembly and fuel pin design and dimensions.

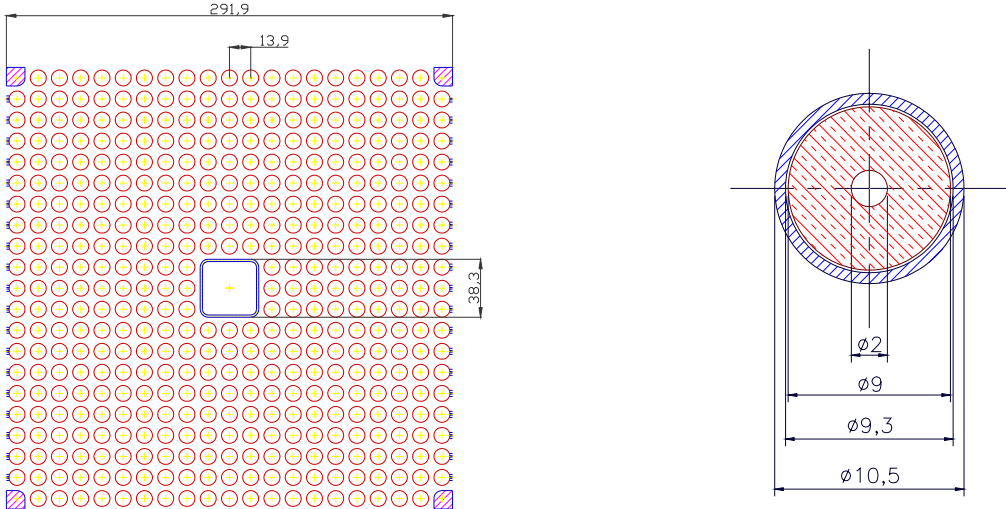


**Fig. 3 – Design and dimensions of fuel assembly and fuel pin [mm]**

## 2.2 Core Power Distribution

The power generated by ELSY reactor is 1500 MWth. At the beginning of cycle (BOC) conditions considered for the present work, the power can be split among the fuel regions: inner, intermediate and outer in about 501, 489 and 492 MWth, respectively. Part of the total power, about 18 MWth, is deposited in the dummy/reflector region and in the structural materials above and below the active core region. This small fraction of power is not taken into account in the present analysis.

The scheme of one quarter of the core with respective fuel assembly (FA) location and its generated power is represented in Fig. 4. This scheme is taken as a reference for the 3D FEM-LCORE modelling in section 4.2.

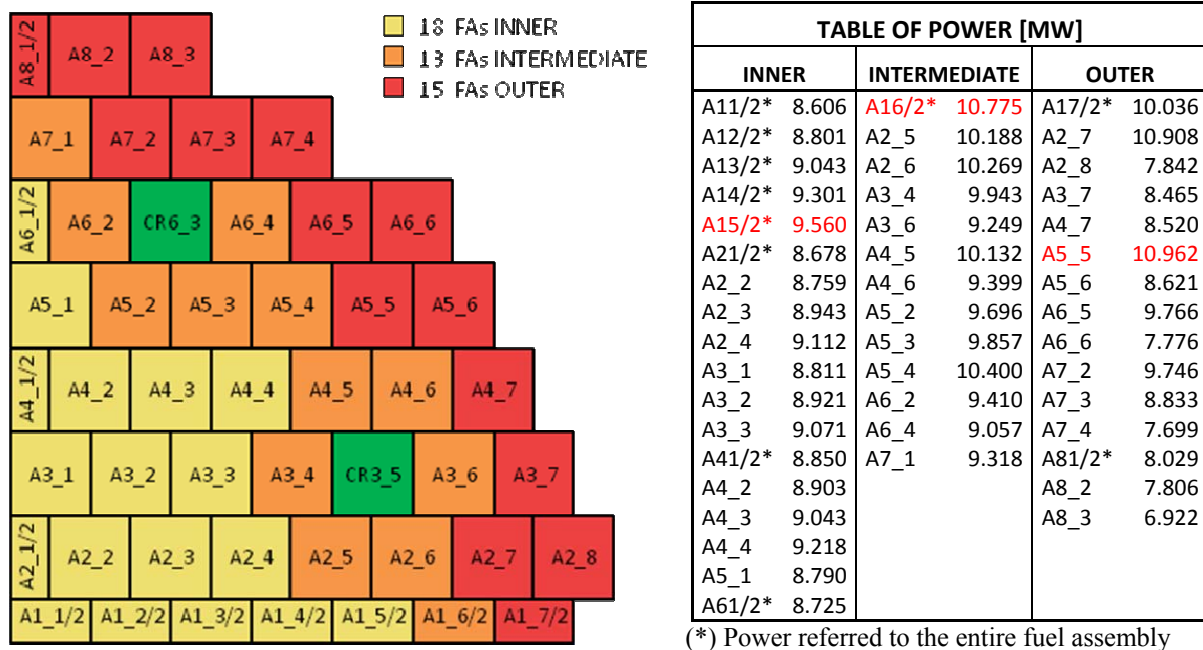


**Fig. 4 – Scheme and labelling of reactor core and power generated in each FA**

The subsequent Tab. 1 summarizes the power produced by ELSY and put in evidence the average power and corresponding radial form factors for each fuel zone. The radial form factor defines the ratio between maximum FA power and average FA power.

	Power [MWth]	#FA	P_avg [MWth]	ffrad
INNER	501.41	56	8.95	1.07
INTERMEDIATE	489.23	50	9.78	1.10
OUTER	491.60	56	8.78	1.25
TOTAL	1482.24	162	9.15	

**Tab. 1 – Power of ELSY Reactor and Radial Form Factors**

The axial power distribution adopted for each fuel zone is shown in Fig. 5 with the corresponding axial form factor.



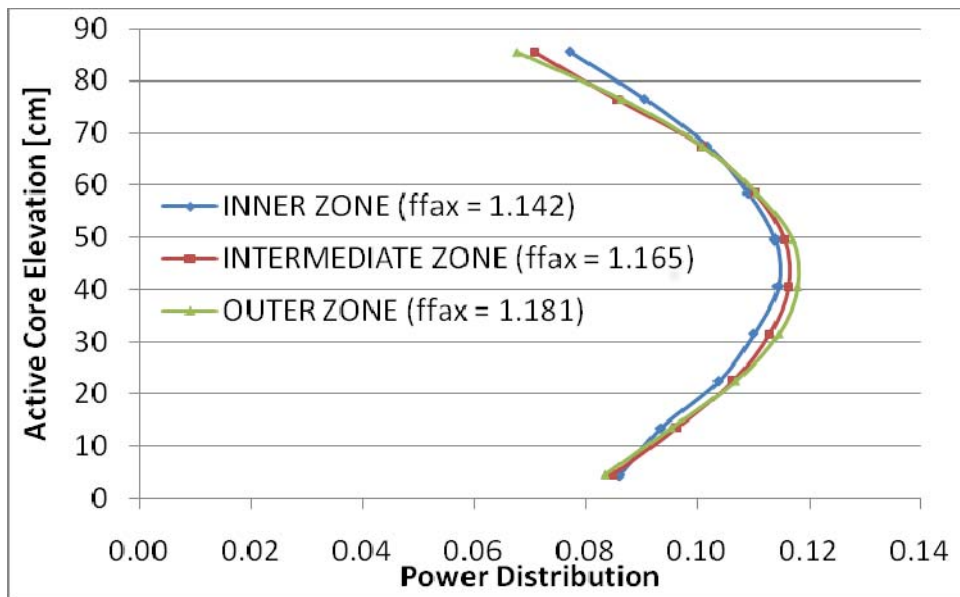


**Fig. 4 – Axial Power Profiles and Form Factors**

For the given core power of 1482.2 MWth and the lead heatup over the core of 80 °C (mixing temperature at core outlet), the lead mass flowrate is fixed to a value of 124540 kg/s over the active core zone.

 <b>Ricerca Sistema Elettrico</b>	<b>Sigla di identificazione</b>	<b>Rev.</b>	<b>Distrib.</b>	<b>Pag.</b>	<b>di</b>
	NNFISS – LP3 - 001	0	L	8	58

### 3. 2D SIMMER-III SIMULATION

At first, a simulation of the thermal-hydraulic behaviour of the primary system of ELSY under steady-state conditions at nominal power has been performed with the 2D SIMMER-III code. The 2D representation of the whole primary circuit is also necessary in order to define the boundary conditions for the detailed analysis of the core thermal-hydraulics with the more refined 3D FEM\_LCORE model presented in section 4.

#### 3.1 The SIMMER-III Code

The SIMMER-III code [3], jointly developed by JAEA (Japan), KIT (Germany), IRSN and CEA (France), is made available to ENEA thanks to an agreement with KIT/Karlsruhe in the frame of a common participation in EU Framework projects such as ELSY. SIMMER-III is a general two-dimensional, three velocity-field, multiphase, multicomponent, Eulerian, fluid-dynamics code coupled with a space-time and energy-dependent neutron transport kinetics model [4]. This code, originally developed for severe accident analysis in sodium cooled fast reactors, is now applicable for the safety analysis of various reactor types with different neutron spectra and coolants, including lead-cooled reactors.

In the present study, the neutronic kinetics model of SIMMER-III was not applied, since the fluid-dynamics analysis of the system is conducted on the basis of the pre-defined core power distribution presented in section 2.2. The overall fluid-dynamics solution algorithm is based on a time-factorization approach, in which intra-cell interfacial area source terms, heat and mass transfers, and the momentum exchange functions are determined separately from inter-cell fluid convection. In addition, an elaborate analytical equation-of-state (EOS) model is available to close and complete the fluid-dynamics conservation equations. A structure model represents the configuration and the time-dependent disintegration of fuel pins and subassembly can walls.

#### 3.2 SIMMER-III Model

The primary system of ELSY plant is modelled in 2D Cylindrical RZ geometry using 27 radial meshes and 61 axial meshes. The SIMMER-III modelling of ELSY is represented in Fig. 5. Axial and radial power profiles in the active core zone are the ones referring to the BOC conditions. The core is represented by seven radial rings for the active zone plus two rings for the reflector and by-pass zone. The core is subdivided in twenty axial meshes; nine of them (from axial mesh 24 to 32) represent the active core. The prolongation of the fuel assembly supporting structure through the upper plenum and the zone above it is also modeled. The eight steam generators are simulated by an annulus of equivalent height and volume and discretized in six radial meshes and ten axial meshes.

The primary pumps are modeled by an imposed pump head of 1.65 bar between two adjacent axial meshes (46 and 47) within the pump duct (radial mesh 12 to 14). Pressure losses through the core due to spacer grids are simulated by equivalent orifice coefficients. In a similar way, the pressure loss of 0.5 bar through the steam generator is reproduced by adequate orifice coefficients. Since the secondary side is not simulated, the heat removal by steam generators is simply modeled by a temperature boundary condition on the tube wall surface.

The detailed SIMMER-III input deck of the ELSY reactor model is listed in Appendix A.

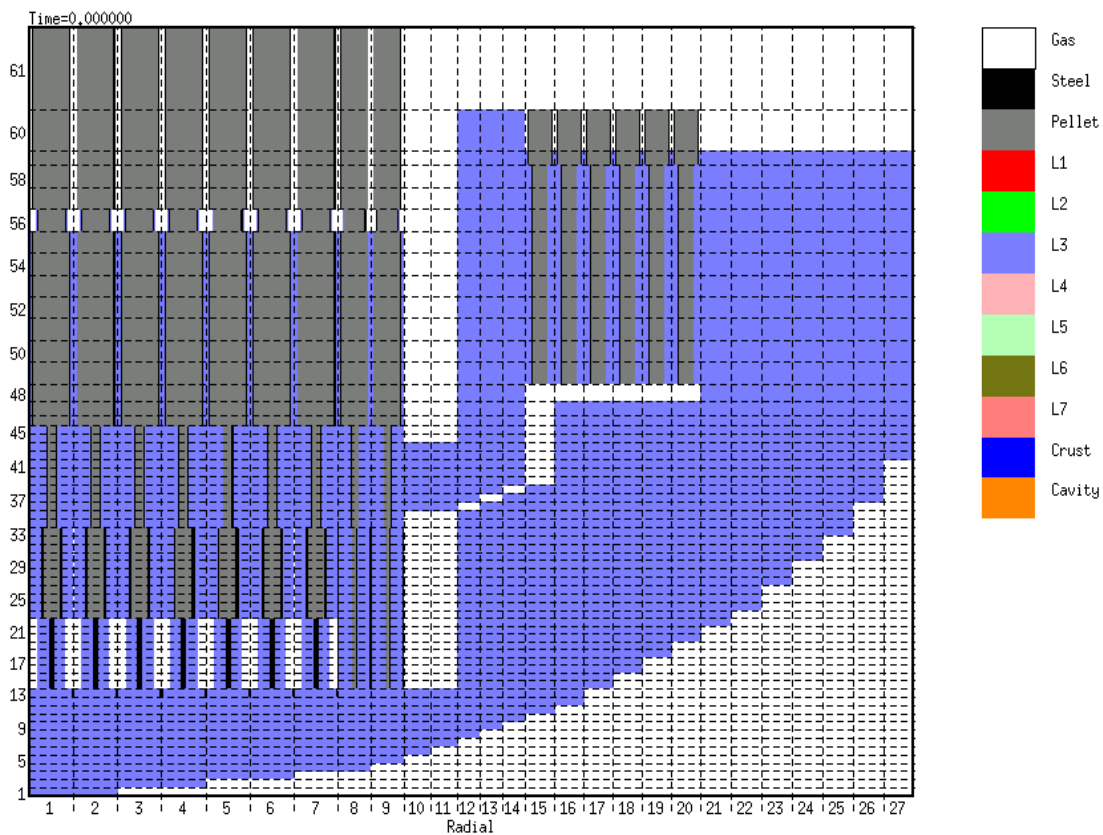


**Fig. 5 – SIMMER-III model of ELSY primary system**

### 3.3 SIMMER-III Results

The steady-state condition at about 1500 MWth power in the primary system is calculated by a transient calculation lasting 200 s, starting from uniform lead temperature of 400 °C in the primary pool. The results of the 2D simulation for the whole primary system are presented first. Secondly, the details of pressure, lead velocity and temperature distributions in the open core are presented and discussed.

#### 3.3.1 Primary System behaviour

The pressure distribution in the primary system is illustrated in Fig. 6. During normal operation, the cover gas is maintained close to atmospheric pressure. Therefore, the pressure in the primary pool increases starting from the free level and moving downwards according to the height of heavy liquid metal, the pressure losses in the circuit. The pressure reaches a maximum at the pool bottom of about 9 bars. The pressure at the core inlet reduces down to about 7.6 bar, according to FA bottom elevation. The total pressure loss through the core due to friction along the FA, the presence of grid spacers and abrupt area change at the core inlet and outlet amounts to approximately 0.9 bar. Owing to this pressure loss and the 1.9 m core height, the pressure at the core outlet reduces down to about 4.7 bar.

A non negligible pressure loss is calculated in the upper plenum due to the presence of FA supporting structures which extend from the core outlet up to the top of the vessel. The radial pressure loss in the upper plenum (about 0.1 bar), which increases from the core centre to the core periphery due to flowing lead, is expected to affect the lead velocity distribution inside the open core. The pumps provide the necessary head (1.65 bar) to circulate the lead in the primary circuit and compensate for a further radial pressure loss of 0.5 bar through the steam generators and remaining losses in the pump duct and primary circuit (about 0.15 bar).

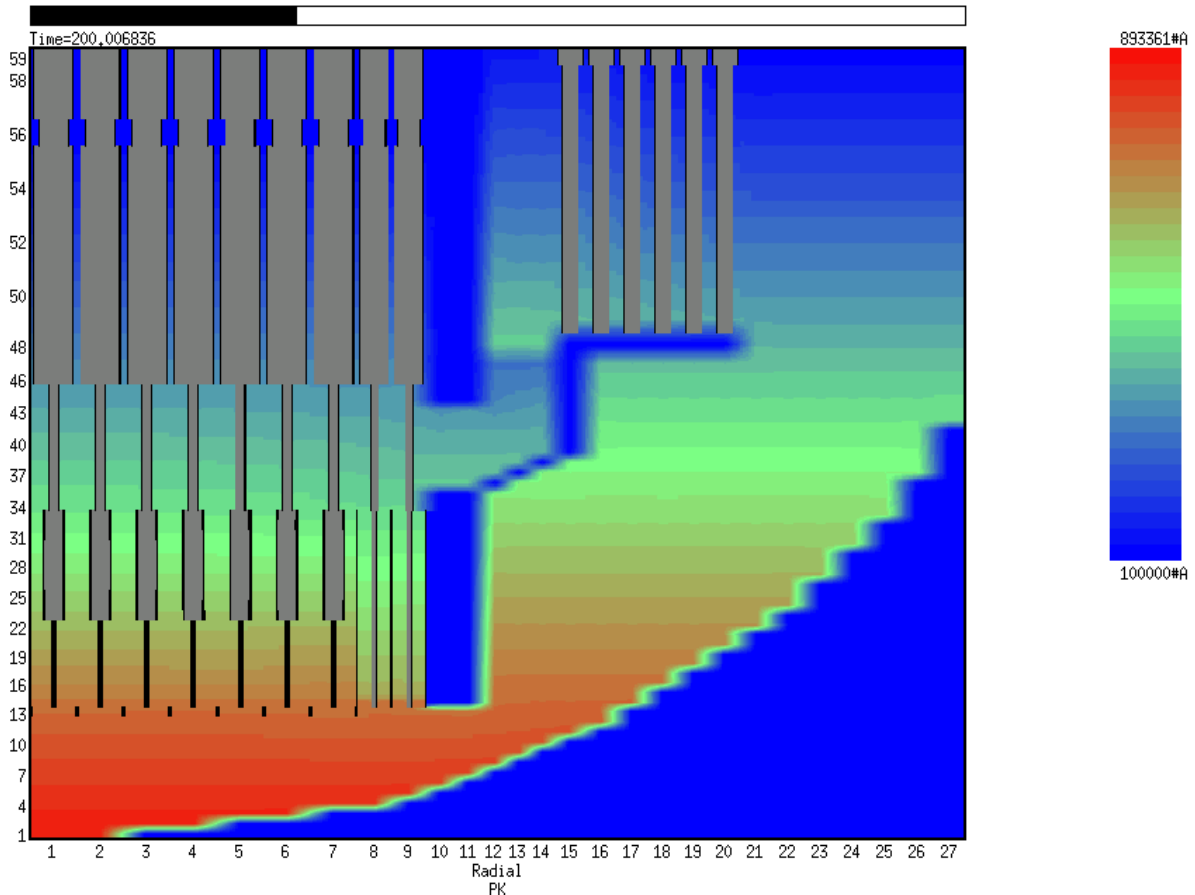


**Fig. 6 – Pressure field in the primary system [Pa]**

The lead velocity distribution in the primary circuit is illustrated in Fig. 7. The primary pumps push the lead inside the steam generators moving the free level upwards. The free level difference between inside and outside (around 0.5 m, see Fig. 2) becomes the driving force for radial lead flow through the steam generators. The cooled lead at the steam generator outlet flows downwards inside the pool towards the core inlet. The lead enters the core lower plenum through the circumferential space left between the core surrounding structure and the vessel wall; then the lead velocity turns round inside the lower plenum towards the core inlet.

Most of the lead (approximately 98%) flows through the FA to remove the active core power, while about 2% of the primary flowrate passes through the reflector assembly and the outer by-pass zone. After heating up in the active core zone, the lead flows out of the core and turns round in the upper plenum towards the pump duct openings, where it is taken by the pumps to close the primary circuit.

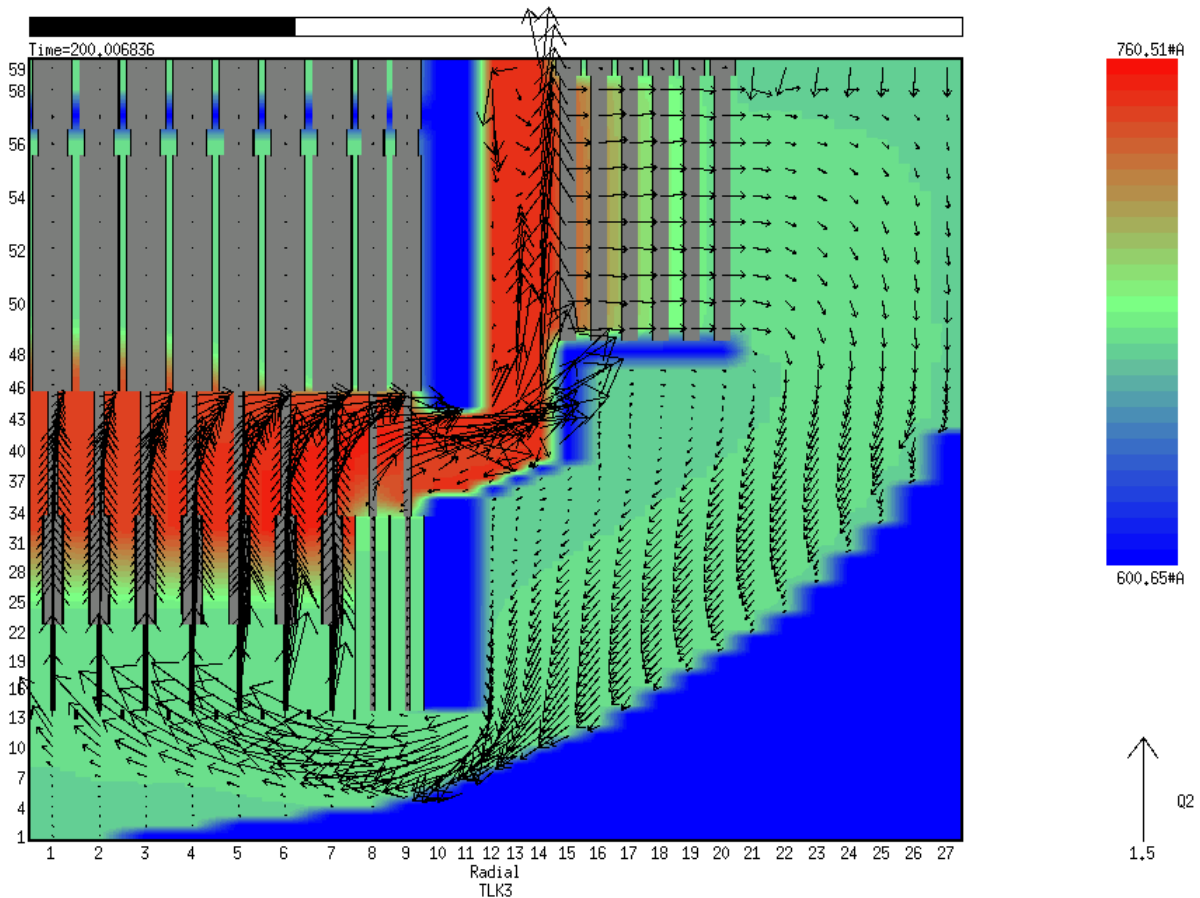


**Fig. 7 – Temperature [K] and velocity [m/s] fields in the primary system**

### 3.1.2 Reactor Core

The fluid-dynamics behaviour of an open core must be carefully analysed since it may significantly affect the presence of hot spots in the core, depending on coolant flow distribution and power peak factors.

In case of wrapped FAs like in SFR cores, a gagging scheme can be applied at the lower grid elevation to regulate the coolant mass flowrate in each FA according to local core power peak factors, thus reducing hot spots and homogenizing the coolant temperature at the core outlet. In case of the ELSY open core the gagging solution cannot, of course, be adopted. Therefore, the right evaluation of flow pattern inside the core is necessary to verify that excessive distortion in the core temperature distribution and related hot spots is avoided.

The pressure and lead velocity distribution in the core calculated by SIMMER-III code is illustrated in Fig. 8. The radial profile of relative pressure at different core elevations (inlet, middle and outlet) is shown in Fig. 9; while the corresponding profiles of vertical velocity is given in Fig. 10. The pressure distribution in the core is influenced by pressure and momentum losses in the lower and upper plenum. At the core inlet, the pressure reduces towards the core periphery along with the lead velocity due to enhanced momentum loss. This perturbation in the lead velocity radial profile attenuates with increasing elevation, thanks to

cross flows through adjacent FAs in the open core, which are induced by the pressure gradient. The maximum velocity calculated at core inlet is 1.8 m/s in radial mesh 5.

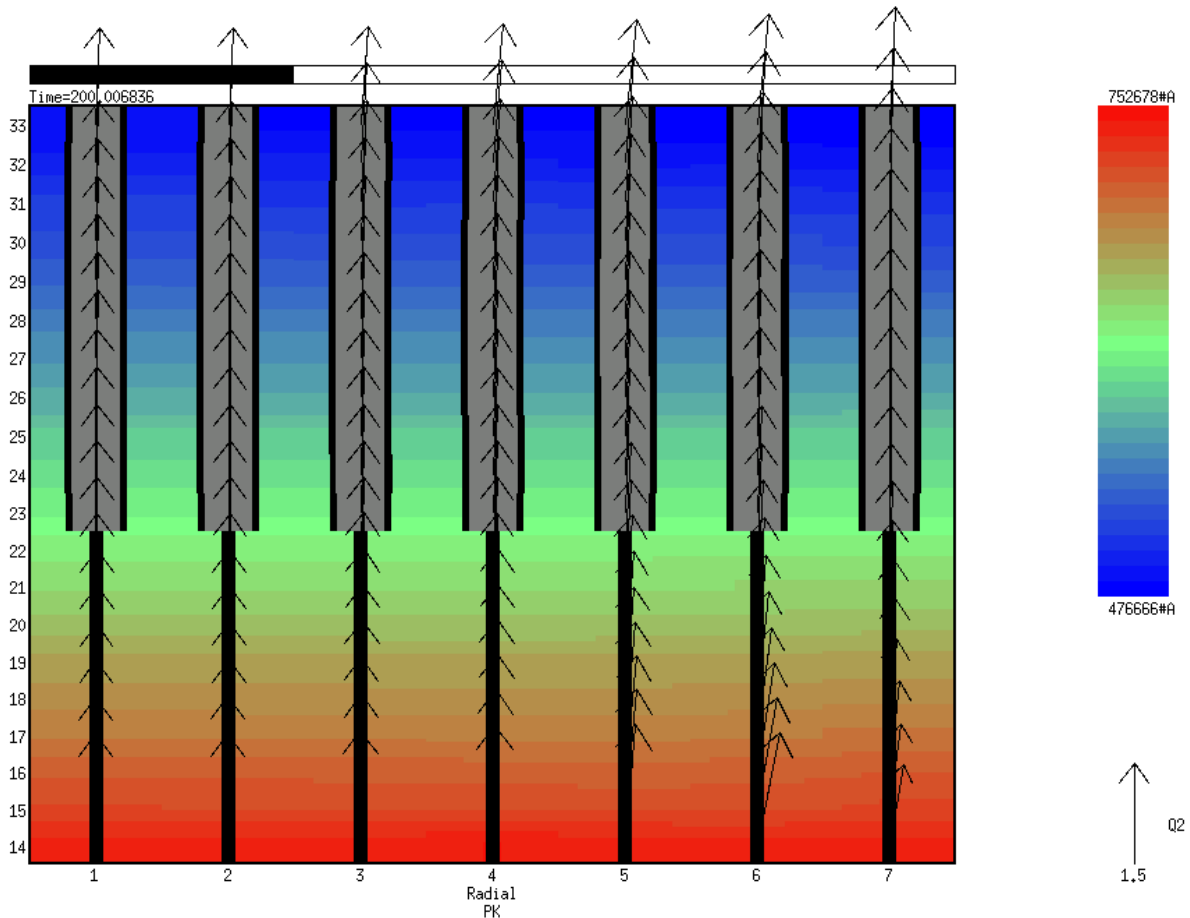


**Fig. 8 – Pressure [Pa] and velocity [m/s] fields in the reactor core**

At middle core elevation which is almost coincident with the active core inlet, both pressure and velocity radial profiles are practically constant as shown in Fig. 9 and Fig. 10, respectively. The lead velocity in the middle core plane approximates 1.6 m/s.

In the upper half of the core (active core) the influence of pressure and momentum losses in the upper plenum becomes significant with consequent lead flow acceleration at the core periphery and corresponding slowing down towards the core centre. The pressure difference over the core radius at the outlet, which is about 0.1 bar (see Fig. 9), is partly determined by friction losses of the lead that flows radially through the upper plenum FA supporting structures, as confirmed by the sensitivity analysis in section 5.4. The vertical lead velocity at the core outlet reaches a maximum value of about 1.8 m/s in the external core region and a minimum value of 1.4 m/s at the core centre (see Fig. 10).

It is worthwhile to note that the maximum lead velocity calculated in the core remains substantially below the 2 m/s value, which is considered to be an upper limit for avoiding significant corrosive effect of the hot lead flow on the fuel rod clad material.

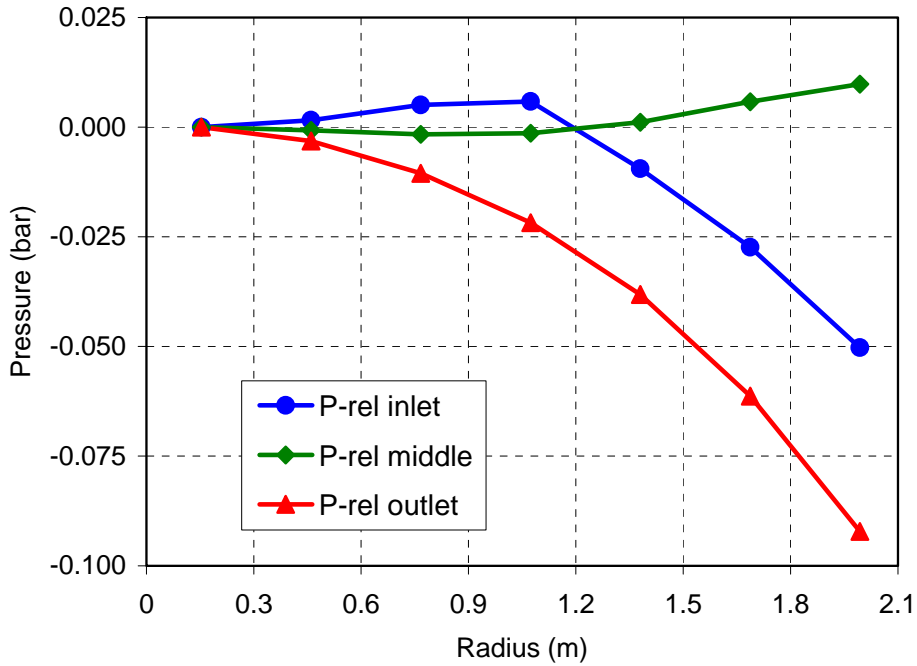


**Fig. 9 – Radial profile of relative pressure at core inlet, middle and outlet**  
(P-rel = 0 at core centre and all elevations)

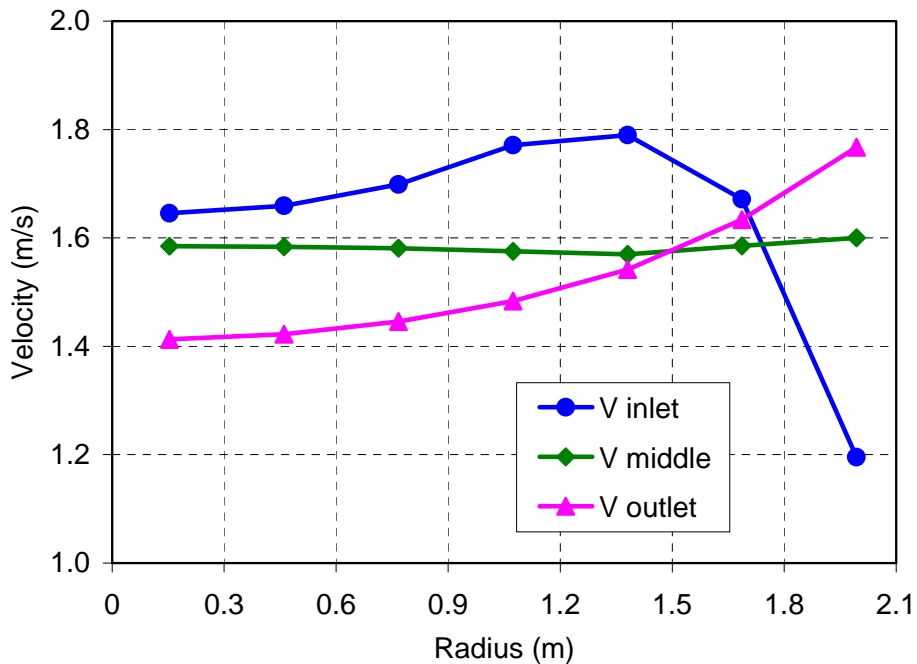


**Fig. 10 – Radial profile of vertical velocity at core inlet, middle and outlet**

The vertical and horizontal velocity fields are illustrated in Fig. 11 and Fig. 12, respectively. The maximum cross flow velocity is equal to 0.4 m/s just above the core inlet (Fig. 12). The cross flows, which are not very significant (below 0.1 m/s) in the central region of the core (between axial mesh 21 and 30), reach a maximum of 0.17 m/s in radial mesh 5 at core outlet.

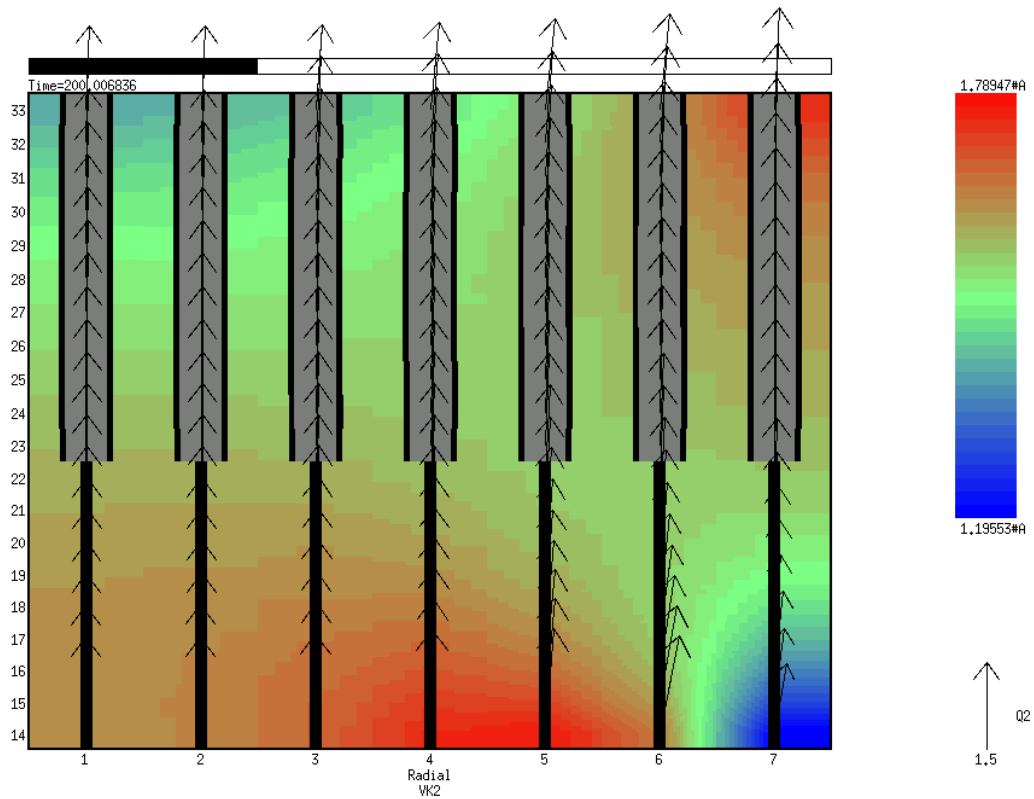


Fig. 11 – Vertical velocity field in the reactor core [m/s]

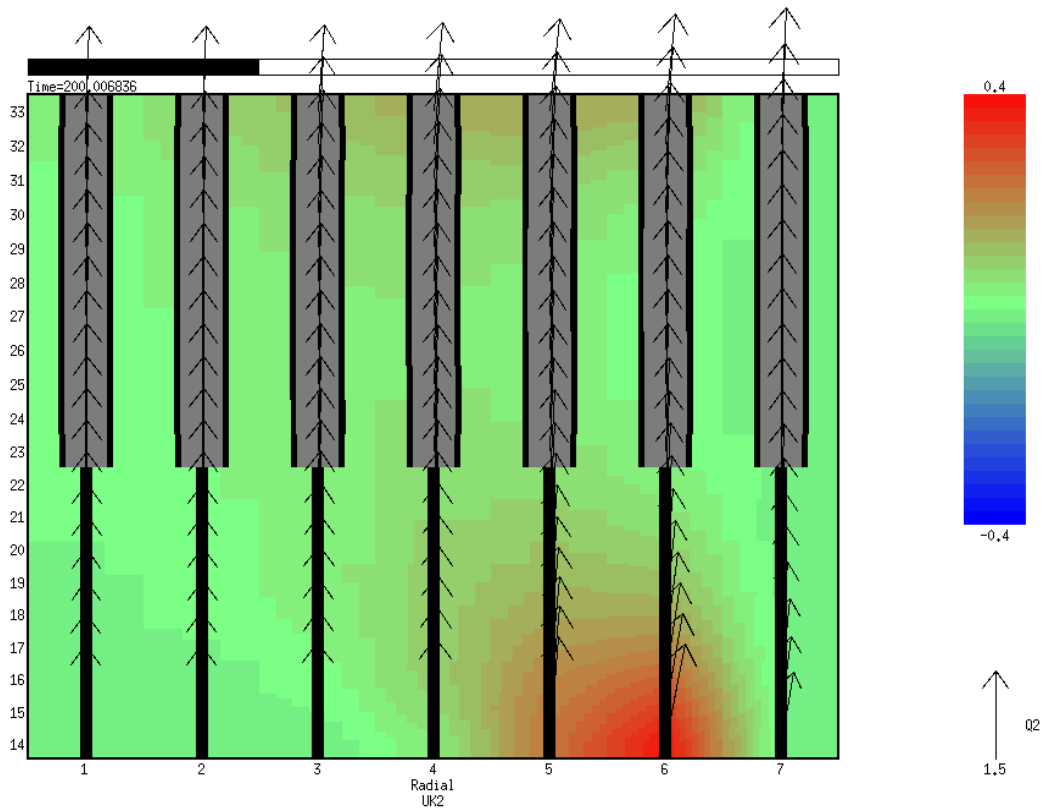
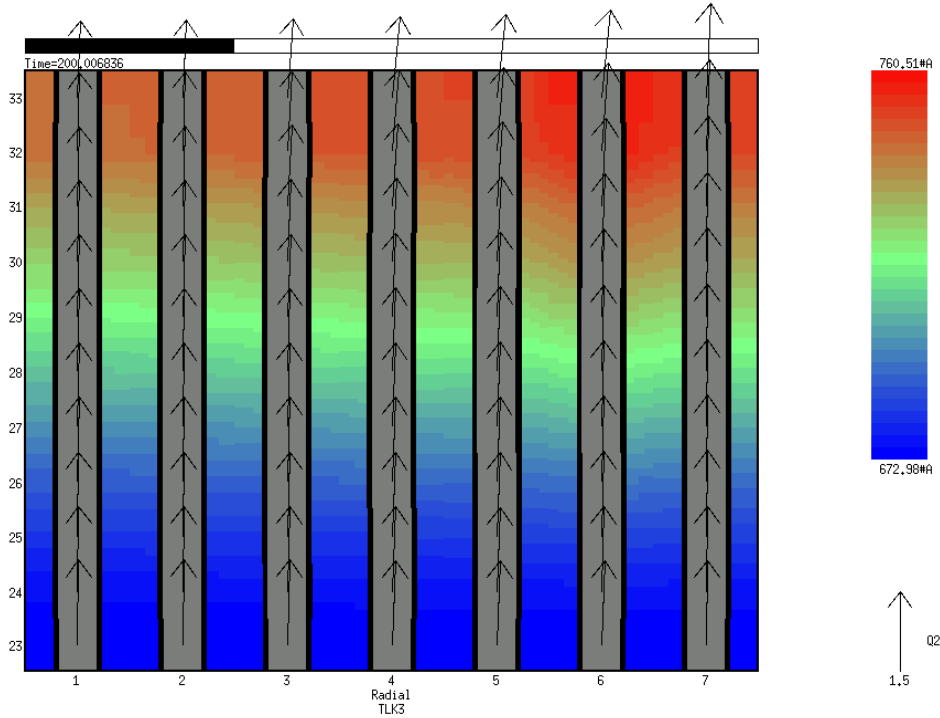


Fig. 12 – Horizontal velocity field in the reactor core [m/s]



The lead and clad temperature distributions in the active core are illustrated in Fig. 13 and 14, respectively. Of course, these temperature fields are influenced by the lead flow redistribution in the active core, as well as axial and radial power peak factors.



**Fig. 13 – Lead temperature distribution in the active core [K]**

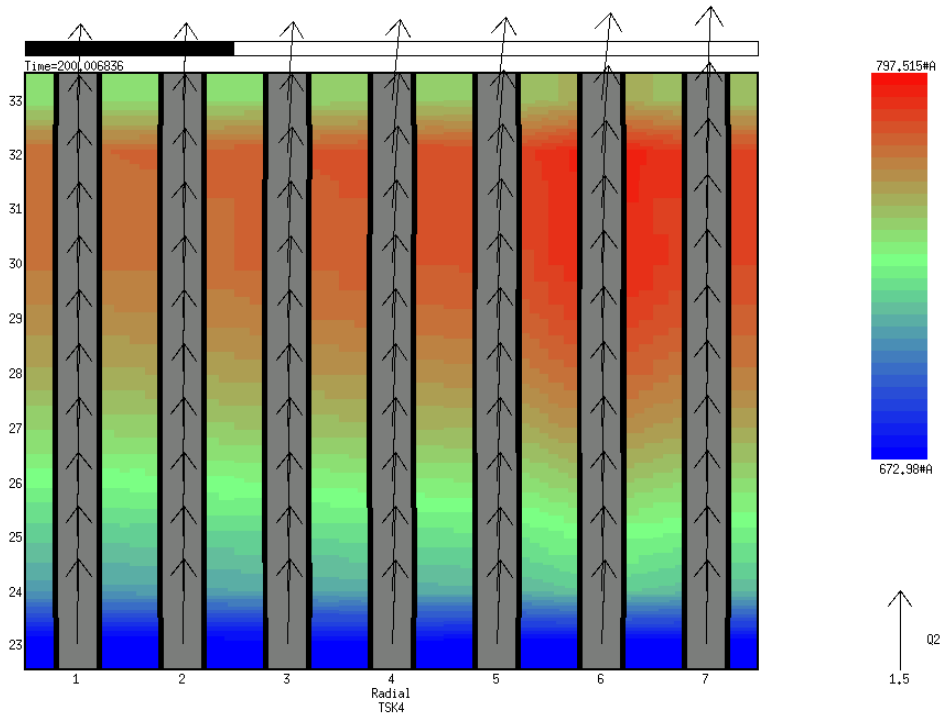


**Fig. 14 – Clad temperature distribution in the active core [K]**

The radial profiles of lead and clad temperatures at core outlet are shown in Fig. 15. The average lead temperature at core outlet is 480 °C. The maximum lead temperature value is 488 °C and is calculated in the radial mesh 6. From the point of view of the core design, there is no concern on the maximum lead temperature reached in the core, since the boiling point of the lead is very high (1743 °C).

Much attention must be paid on the maximum clad temperature reached at the active core outlet, since it is limited to 550 °C under normal operation due to constraints relevant to clad material corrosion problems at higher temperatures. As shown in Fig. 15, the mean  $\Delta T$  between lead and clad calculated by the code, which implements standard convective heat transfer correlations applicable to liquid metal environment, is around 30-40 °C. The maximum clad temperature calculated in the radial mesh 6 is about 525 °C, therefore, with a margin of 25 °C below the clad temperature safety limit reported above.

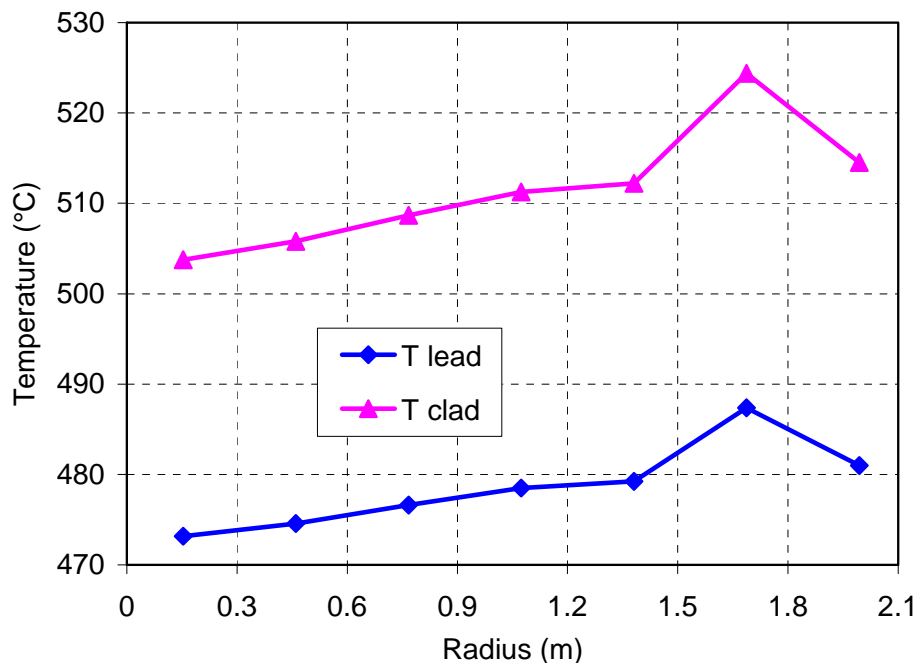


**Fig. 15 – Radial profile of lead and clad temperature at core outlet**

The present analysis has been conducted at BOC conditions under which the radial peak factor exhibits the maximum value towards the core periphery where the lead velocity is above the mean value, thus reducing the amplitude of clad hot spots in the core. The situation might be different at EOC conditions, in which the radial peak factor reaches its maximum at the core centre, where the lowest lead velocity values are calculated.


However, the assessment of different fuel cycle conditions and clad temperature safety limits is out of the scope of this report; therefore, the BOC conditions are mainly taken as the representative case for code benchmarking on fluid-dynamic behaviour of the open ELSY core.

The axial profile of lead and clad temperatures in the hottest radial mesh 6 is given in Fig. 16. The maximum lead-clad  $\Delta T$  is about 60 °C in the active core middle plane (1.4 m above the

core bottom) according to axial power distribution. However, the maximum clad temperature of 525 °C is calculated at the top of the active core at 1.8 m elevation.

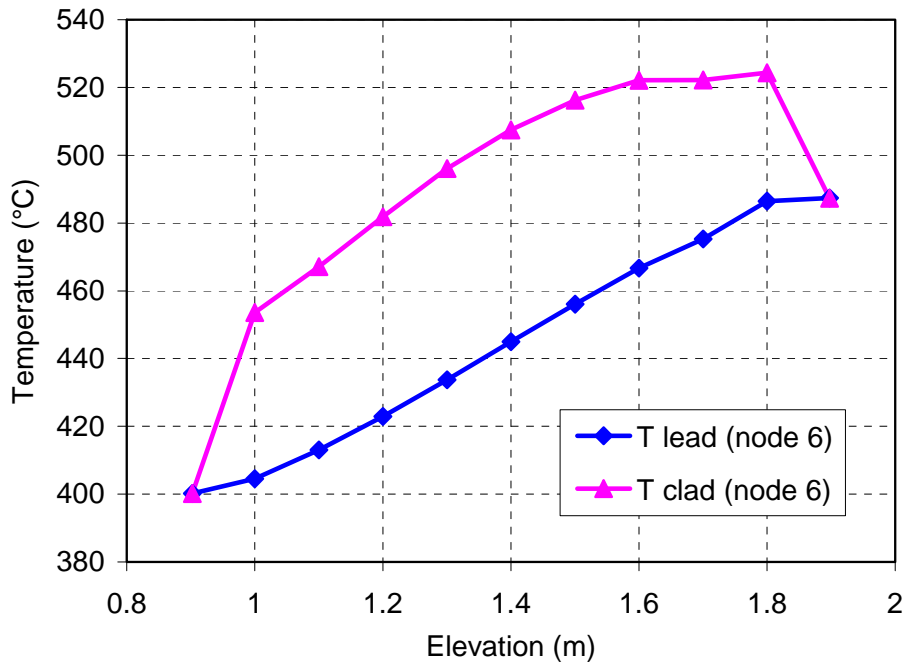


**Fig. 16 – Axial profile of lead and clad temperature (radial mesh 6)**

 <b>Ricerca Sistema Elettrico</b>	<b>Sigla di identificazione</b>	<b>Rev.</b>	<b>Distrib.</b>	<b>Pag.</b>	<b>di</b>
	NNFISS – LP3 - 001	0	L	18	58

## 4. 3D FEM-LCORE SIMULATION

This section of the report describes the results of the simulation of the thermal-hydraulic behaviour of the open square core of ELSY, under steady-state conditions at nominal power, performed by the University of Bologna with the 3D FEM-LCORE code developed in collaboration with ENEA in the frame of previous ENEA-MSE research program.

This simulation with the FEM-LCORE code, which is limited to the reactor core and lead lower/upper plenum, takes advantage from the SIMMER-III analysis presented in section 3 for setting up the conditions of pressure and lead velocity at the boundaries of the calculation domain.

### 4.1 The FEM-LCORE Code

The 3D CFD FEM-LCORE code [5] has been developed with the purpose of analyzing the thermal-hydraulic behaviour in liquid metal reactors. The purpose of this code is to investigate three-dimensional pressure, velocity and temperature fields inside nuclear reactors at the coarse fuel assembly level. All the sub-channel details are summarized by parametric coefficients. Due to the complexity of the geometry, approximate CFD models have been developed for the core region, for the upper and lower plenum and for subassembly computations.

The solution of the Navier-Stokes system and the energy equation is obtained by using the finite element method. The numerical simulations take place at a coarse, assembly length level and are linked to the fine, sub-channel level state through transfer operators based on parametric coefficients that summarize local fluctuations. The overall effects between assembly flows are evaluated by using average assembly turbulent viscosity and energy exchange coefficients. The reactor upper and lower plenum region model is introduced by coupling the Navier-Stokes and energy system with a turbulence model. The  $\kappa - \epsilon$ ,  $\kappa - \omega$  and LES turbulence models have been implemented in the finite element code.

Meshing tools are available in the code to design the reactor geometry and to configure the solver class for Navier-Stokes, energy and turbulence models. The distribution of the core power factors and pressure losses are introduced by using external files which can be generated automatically by appropriate tools.

### 4.2 FEM-LCORE Model

The reactor FEM-LCORE model [6] depicted in Fig. 17 has been prepared starting from the horizontal one-quarter section schematized in Fig. 4 of section 2.2. The fuel assembly consists of  $n \times n$  pin lattice resulting in 170 positions fitting the required core area in an approximately circular arrangement. The model design distributes the fuel assemblies in three zones: 56 fuel assemblies in the inner zone, 62 fuel assemblies in the intermediate zone and the remaining 44 fuel assemblies in the outer zone. The power distribution factors are the ones indicated in Fig. 4. The maximum peak factor is 1.17, while the minimum one is 0.74. The fuel assembly configuration is not based on a Cartesian grid but rather over a staggered grid.

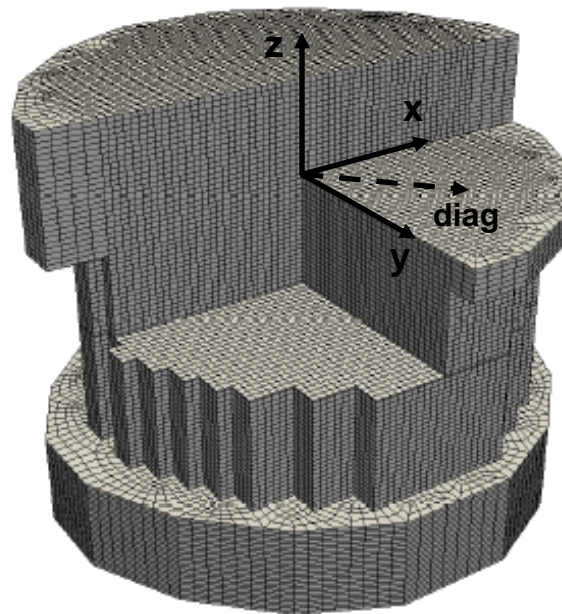


**Fig. 17 – Computational three-dimensional reactor model**

The reactor is cooled by lead which enters at the temperature of 400 °C. The computational domain (see Fig. 17) includes the active (upper core) and not active core section (lower core) and the upper and lower plenum. In the computational description the core region is considered from 0.0 m to 1.85 m where the active core ranges between  $H_{in} = 0.95$  m and ends at  $H_{out} = 1.85$  m. Below the core there is the lower plenum with the inlet between -0.9 m and 0.0 m. The lower plenum has an approximate spherical shape with the lowest region at -1.2 m. Over the core, for a total of 1.2 m, there is the upper plenum with the coolant outlet. The heat generation zone or the active core zone for the reactor starts at  $H_{in} = 0.95$  m and ends at  $H_{out} = 1.85$  m. Since the model describes the reactor at assembly level the sub-assembly composition is seen as a homogeneous medium; in particular the coolant assembly ratio is 0.548. Each assembly has a square shape with the side length of  $L = 0.294$  m. The open assembly model is obtained by imposing the velocity fields parallel to the z-direction at the core inlet (like in the 2D SIMMER-III model) and solving the complete three-dimensional core system over the rest of the core reactor.

Boundary conditions (pressure and lead velocities) at the entrance into the lower plenum and at the exit from the upper plenum are taken according with the SIMMER-III results for the overall primary system presented in section 3.3.1. The exit from the upper plenum in the reactor consists of eight circular-shape pump duct openings, which are simulated with respective rectangular-shape openings in the FEM-LCORE model.

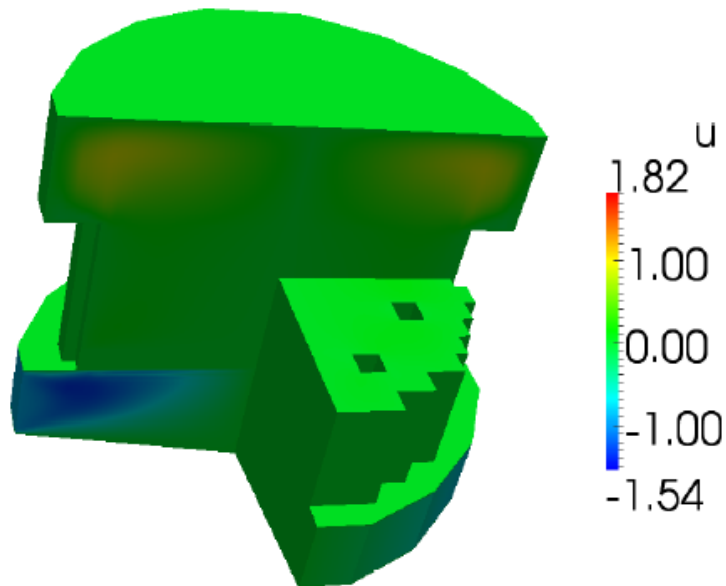
Detailed information on preparation of the input deck and definition of the initial and boundary conditions for the 3D reactor model are given in Ref. [5, 6].

### 4.3 FEM-LCORE Results

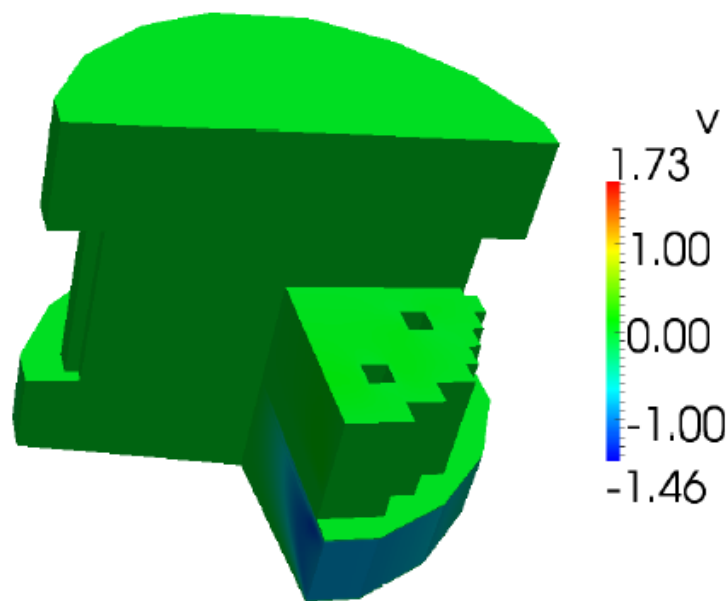
The results of the 3D simulation for the overall calculation domain are illustrated first. Secondly, the details of the pressure, lead velocity and temperature distributions in the open core are illustrated and discussed.

### 4.3.1 Overall Calculation Domain

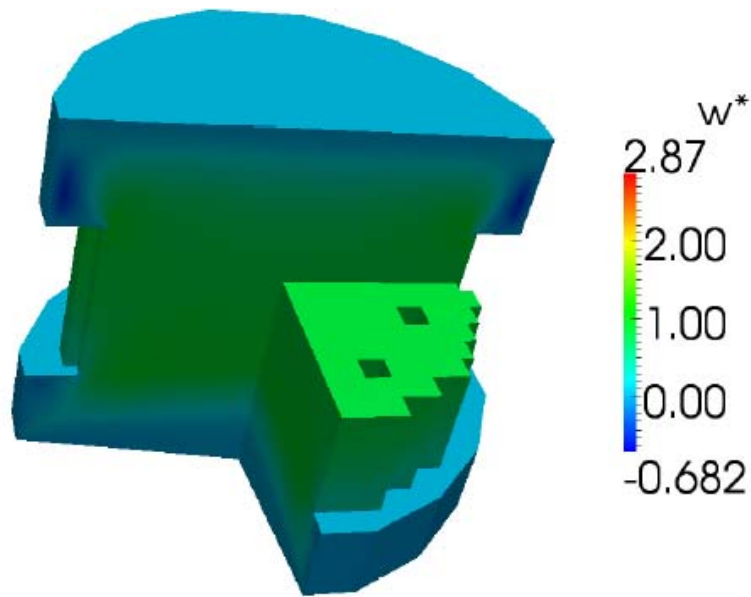
An overview of the lead velocity distribution in the overall calculation domain is given from Fig. 18 to Fig. 20 for the three Cartesian directions: u component on the x-axis, v component on the y-axis and w component on the z-axis.



**Fig. 18 – Lead velocity u component distribution in the overall calculation domain [m/s]**



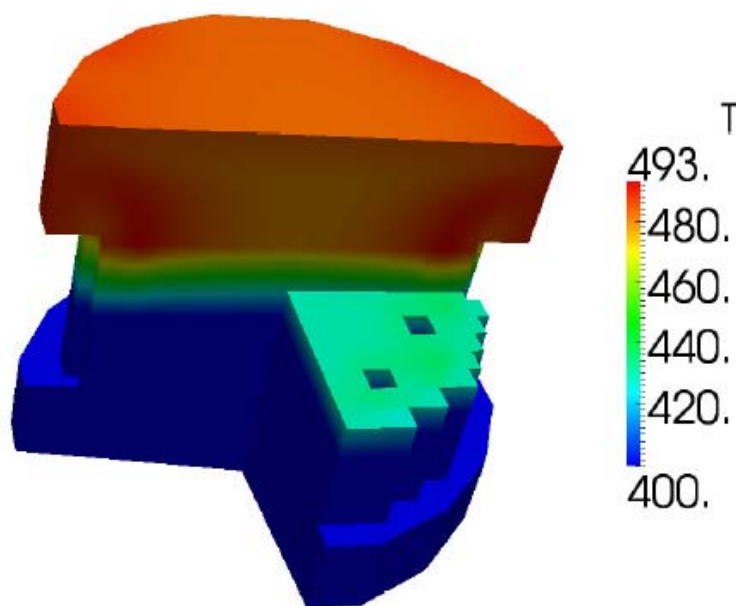
**Fig. 19 – Lead velocity v component distribution in the overall calculation domain [m/s]**



**Fig. 20 – Lead velocity  $w$  component distribution in the overall calculation domain [m/s]**

Noticeable horizontal lead velocity values ( $u$  and  $v$  components) are observed at the entrance in the lower plenum; the maximum value is close to 1.5 m/s. The horizontal  $u$  component reaches high values up to 1.3 m/s in the upper plenum, since there is a pump duct opening located in the  $x$  direction, but not in the orthogonal  $y$  direction, where the velocity ( $v$  component) is limited. Of course, the vertical lead velocity ( $w$  component) reaches the highest values in the core region.

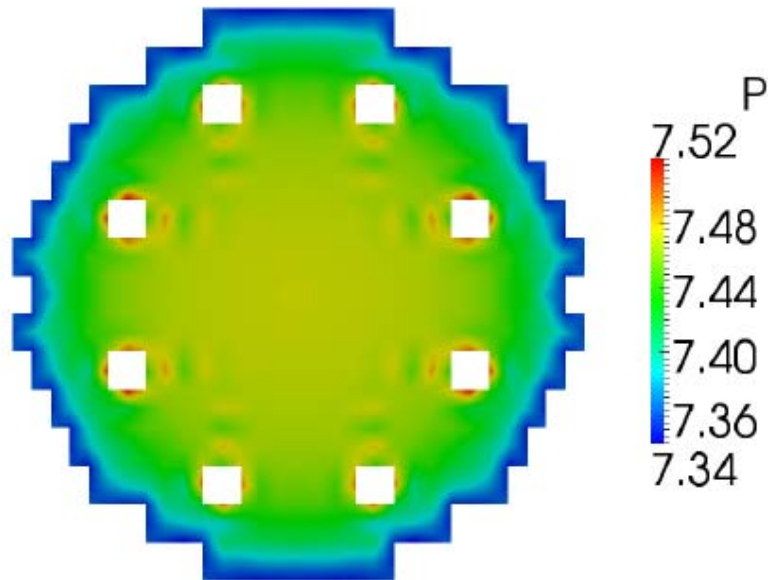
Fig. 21 gives an overview of the lead temperature distribution in the overall calculation domain. The hot lead flows out of the core at different temperatures according to nuclear power distribution and partially mixes in the upper plenum, before leaving it through the pump duct openings.



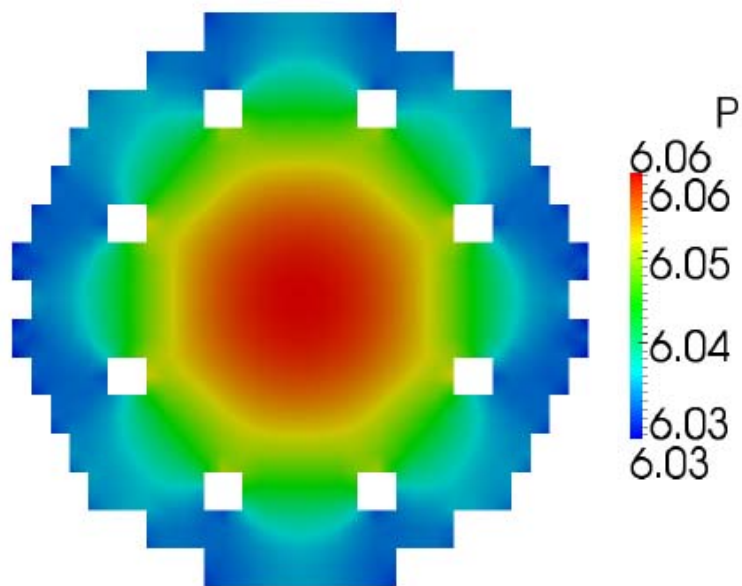
**Fig. 21 – Lead temperature distribution in the overall calculation domain [°C]**

### 4.3.2 Reactor Core

The pressure distribution calculated by the FEM-LCORE code at different core inlet, middle and outlet z-planes is illustrated from Fig. 22 to Fig. 24. The pressure profiles in different horizontal directions (x, y and the diagonal one) at the same elevations are shown from Fig. 25 to Fig. 27.

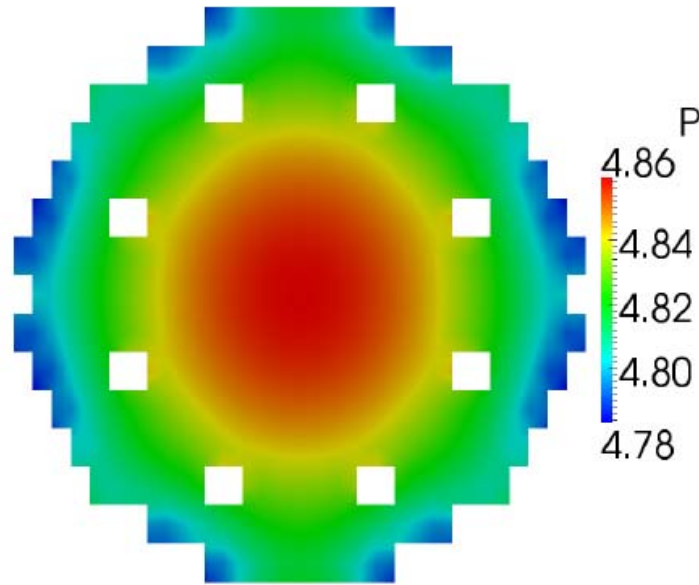


**Fig. 22 – Pressure distribution at core inlet z-plane [bar]**



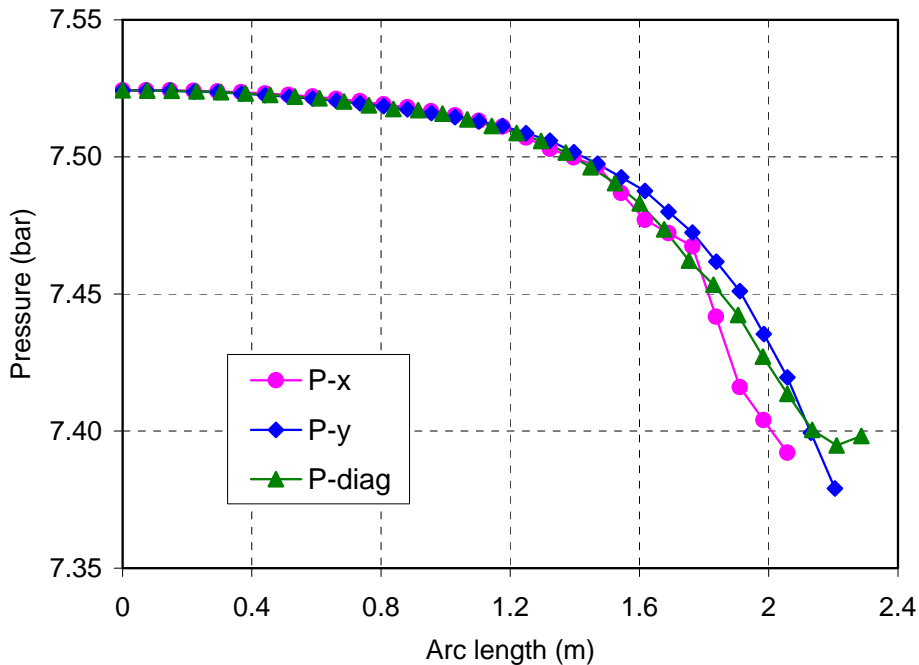
**Fig. 23 – Pressure distribution at core middle z-plane (onset of active zone) [bar]**





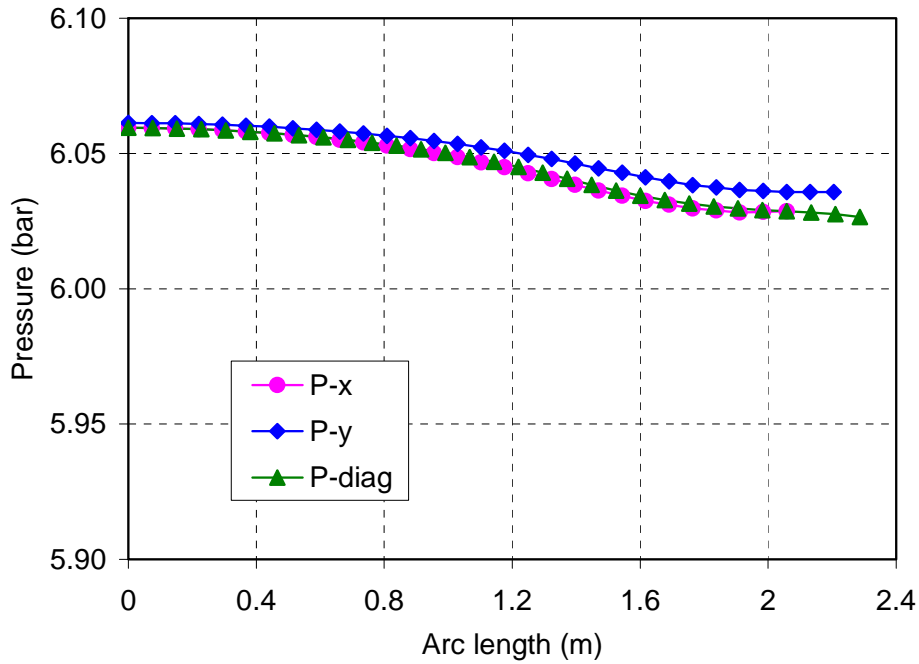
**Fig. 24 – Pressure distribution at core outlet z-plane [bar]**

The pressure gradient over the core inlet z-plane, mainly induced by turbulent flow effects in the lower plenum, does not differ significantly in different directions (see Fig. 25). The maximum value over the mean core radius length ( $R_c = 2.2$  m) is approximately 0.15 bar.



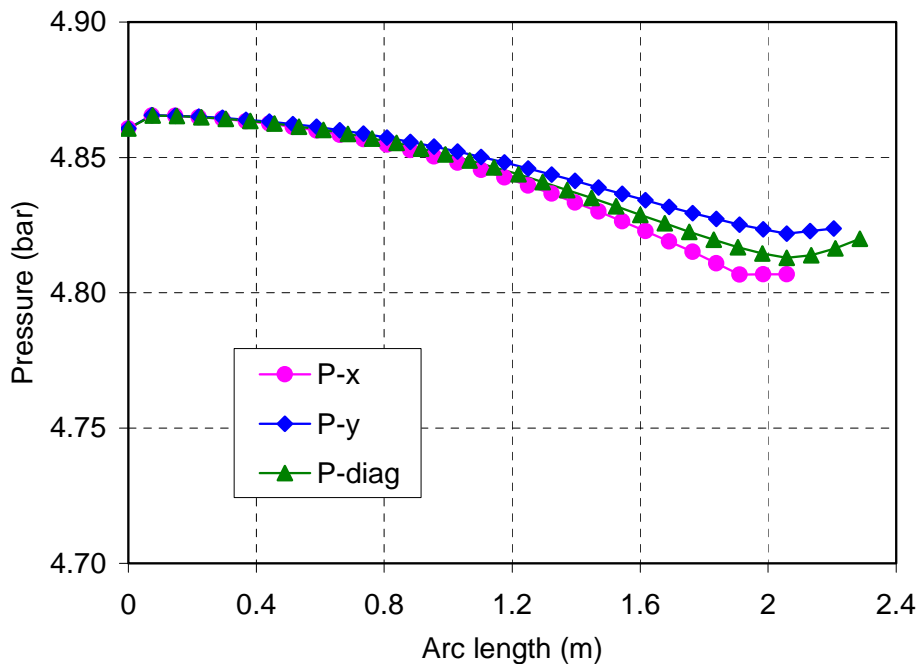
**Fig. 25 – Radial pressure profiles at core inlet z-plane (x, y, and diagonal directions)**

The maximum pressure gradient over the core radius reduces down to about 0.04 bar at the middle core z-plane (see Fig. 26), owing to cross-flows and then lead flow redistribution in the not active lower half of the core. A slight deviation of pressure trend observed in the y direction could be correlated to asymmetric position of upper plenum pump duct openings.



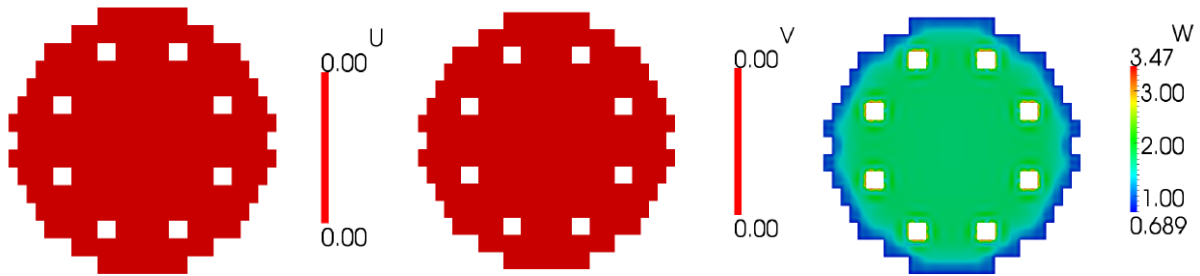
**Fig. 26 – Radial pressure profiles at core middle z-plane (x, y, and diagonal directions)**

The pressure gradient over the core radius increases up to a maximum of about 0.065 bar at the core top (see Fig. 27), owing to turbulent flow effects in the upper plenum and flow redistribution in the active upper half of the core. It is worthwhile to note here that upper plenum FA supporting structures are not modelled with FEM-LCORE and then the pressure gradient is surely underestimated. The pressure trend deviations in the various directions are likely correlated to the asymmetric position of pump duct openings at the upper plenum exit.

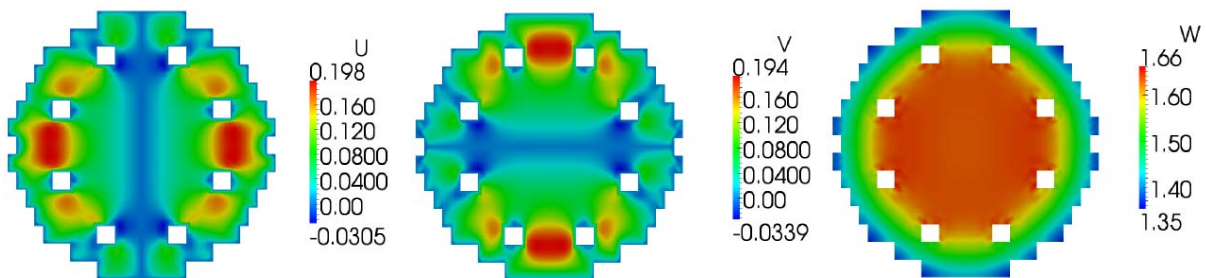


**Fig. 27 – Radial pressure profiles at core outlet z-plane (x, y, and diagonal directions)**

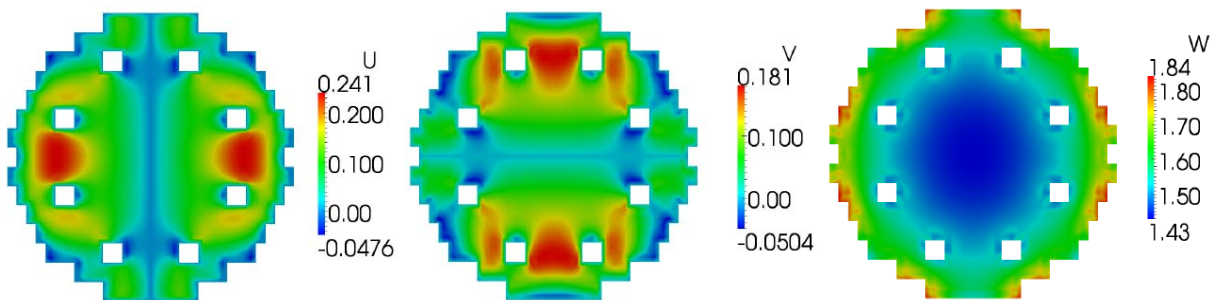
The distribution of lead velocity components at core inlet, middle and outlet z-planes is illustrated from Fig. 28 to Fig. 30. The radial profiles of vertical velocity at core inlet, middle and outlet z-planes are shown from Fig. 31 to Fig. 33 for the three directions x, y and the diagonal one.



**Fig. 28 – Lead velocity distribution at core inlet z-plane [m/s]**



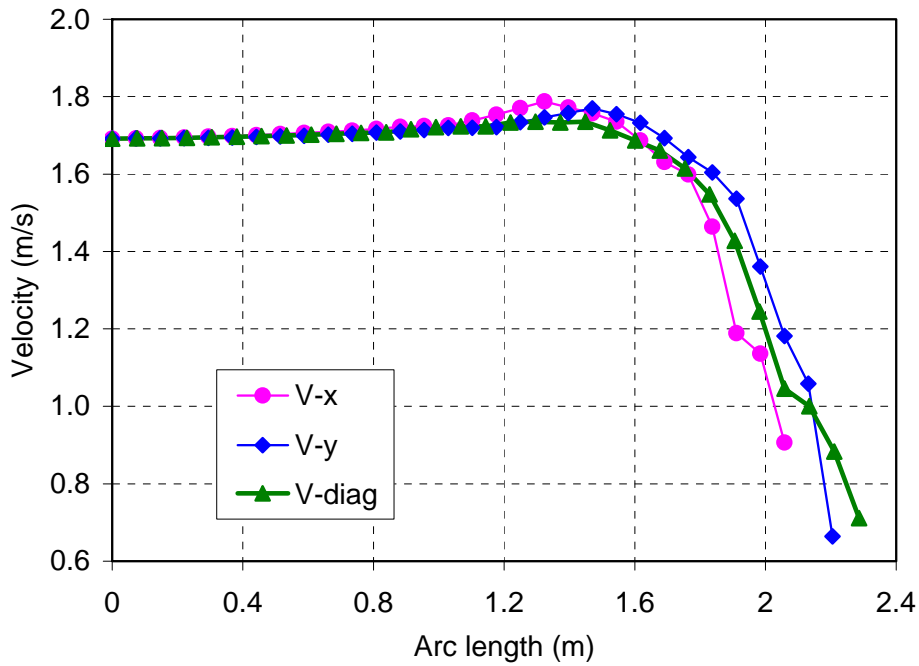
**Fig. 29 – Lead velocity distribution at core middle z-plane (active core inlet) [m/s]**



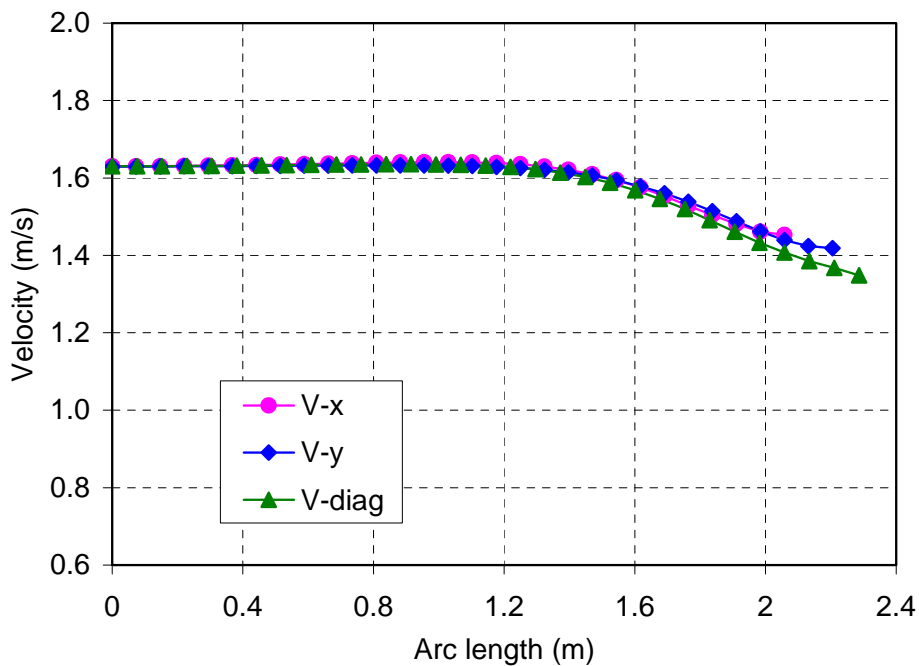
**Fig. 30 – Lead velocity distribution at core outlet z-plane [m/s]**

At the core inlet z-plane the velocity components  $u$  and  $v$  are assumed equal to zero due to bottom FA structure constraints (see Fig. 28). The cross flow velocities reach a maximum of about 0.2 m/s at the core middle z-plane (Fig. 29) and a maximum of 0.24 m/s at the core outlet z-plane in the x direction (Fig. 30).

The vertical velocity at the core inlet z-plane is almost constant over the 0.0 - 1.5 m radius range and reduces significantly towards the core periphery in all horizontal directions (see Fig. 31). The maximum velocity value remains below 1.8 m/s, while the minimum value is 0.66 m/s in the y direction.



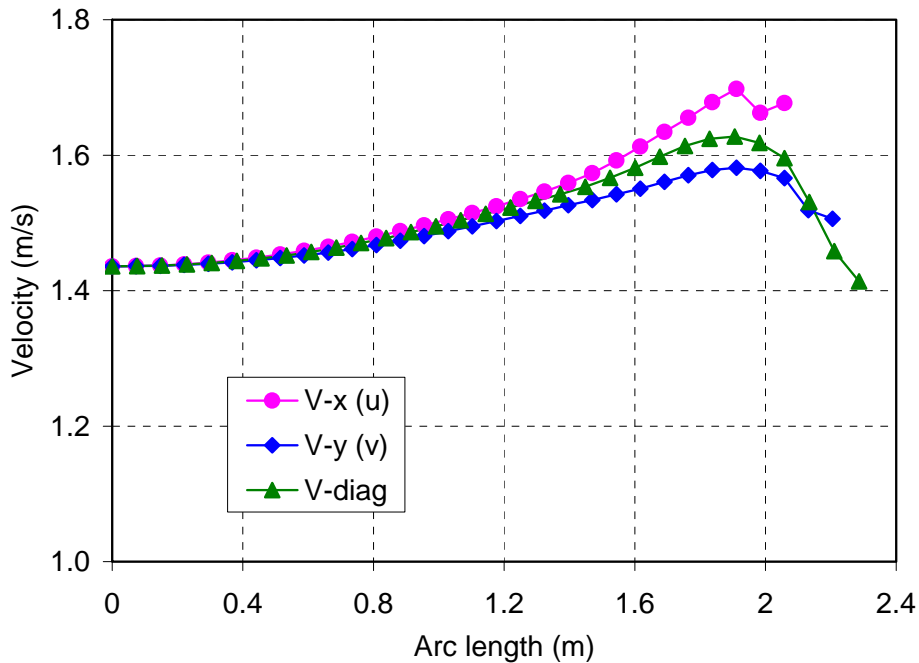
**Fig. 31 – Radial profiles of lead vertical velocity at core inlet z-plane**  
(x, y, and diagonal directions)



**Fig. 32 – Radial profiles of lead vertical velocity at core middle z-plane**  
(x, y, and diagonal directions)

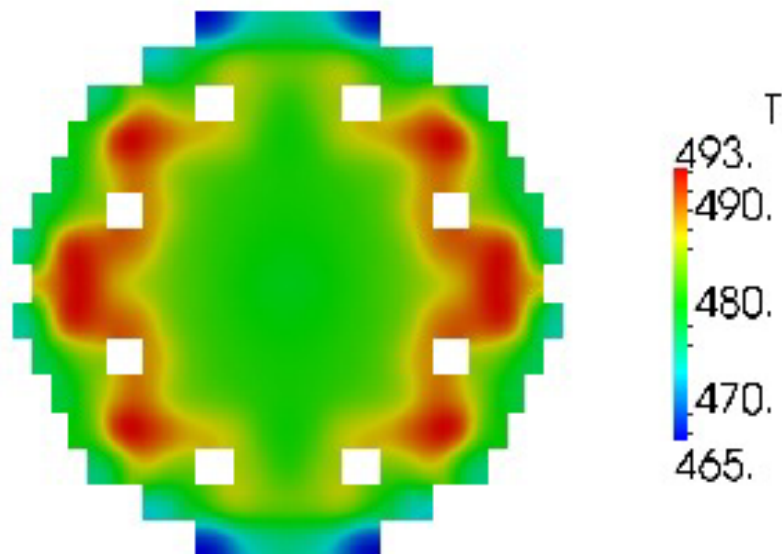
No significant deviation is observed in the vertical velocity profile at core middle z-plane in the three directions (see Fig. 32). Some deviation in the vertical velocity trend is observed at the core outlet z-plane mainly due to asymmetric location of the pump duct openings (see Fig.

33). The vertical velocity is 1.44 m/s at core centre and progressively increases towards the core periphery reaching a maximum of 1.7 m/s in the x direction.



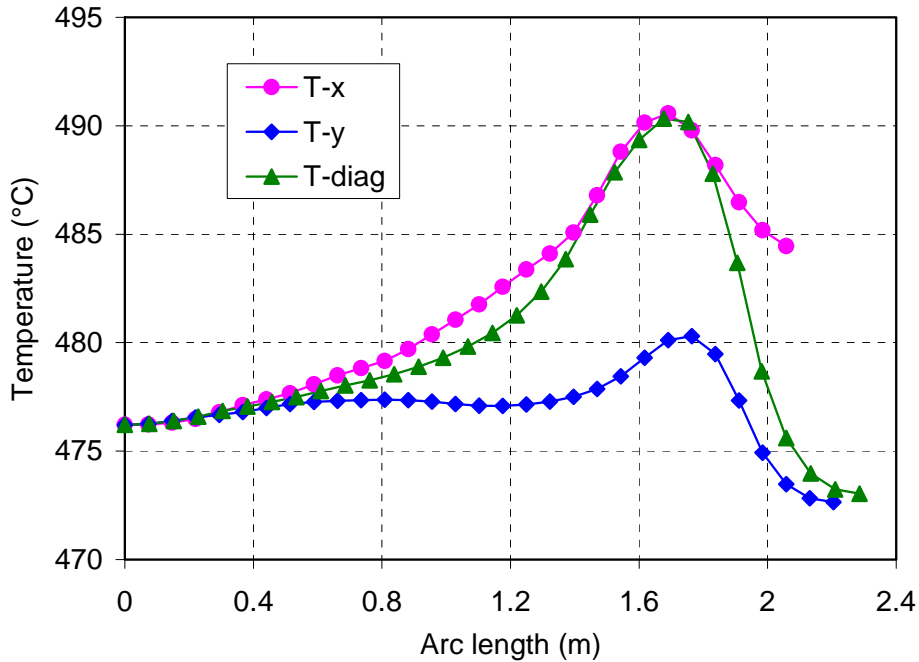
**Fig. 33 – Radial profiles of lead vertical velocity at core outlet z-plane (x, y, and diagonal directions)**

Fig. 34 gives an overview of the lead distribution at the core outlet z-plane. Significant circumferential asymmetries are evidenced, with enhanced hot spots located towards the core periphery, according to the greatest FA power values. The lead temperature at core outlet reaches a maximum of 493 °C near the x direction, while the minimum value is 465 °C in the external core region around the y direction.



**Fig. 34 – Lead temperature distribution at core outlet [°C]**

The radial profile of lead temperature at the core outlet z-plane in the three directions is shown in Fig. 35. As observed before, the largest hot spots are evidenced around core radius  $R_c = 1.7$  m in both x and diagonal directions. The axial temperature profile in the hot spot zone of the x and y directions in shown in Fig. 36.



**Fig. 35 – Radial profiles of lead temperature at core outlet z-plane (x, y, and diagonal directions)**

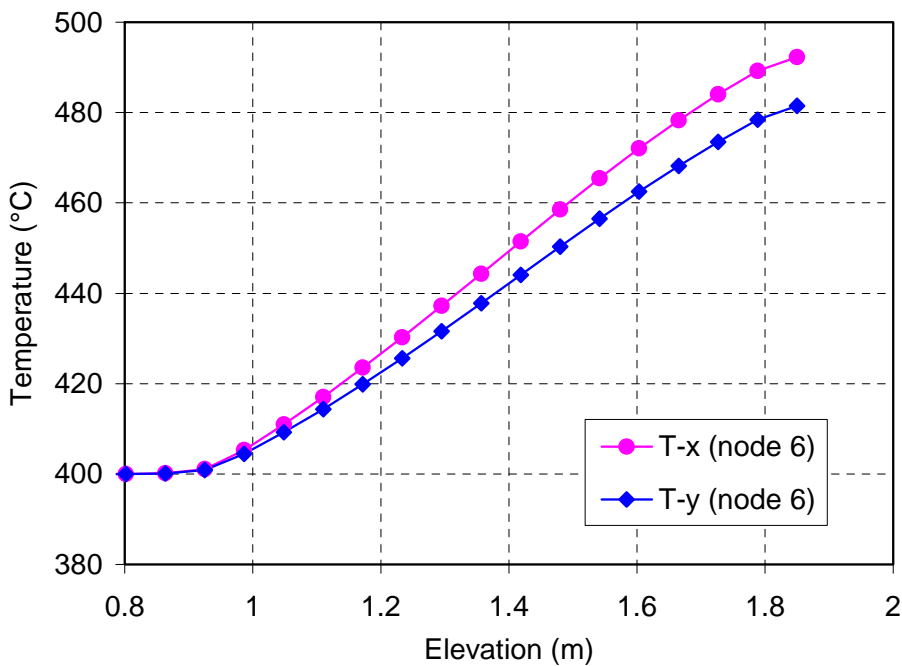


**Fig. 36 – Axial profiles of lead temperature at  $R_c = 1.7$  m (x and y directions)**

## 5. SIMMER-III AND FEM-LCORE RESULT COMPARISON

In this section, the results of the FEM-LCORE model are compared with the ones of the SIMMER-III model for code validation purposes.

The geometrical data for the common computational domain and the initial conditions for the two code models have been harmonized, in order to best compare the calculation results. However, some differences between the two models remain; in particular, the presence of FA supporting structure in the upper plenum is neglected in the 3D FEM-LCORE model. The comparison of the results for the open square core region is illustrated from section 5.1 to 5.3. The influence of upper plenum FA supporting structures on code results is investigated in section 5.4.

### 5.1 Core Pressure

The radial pressure profiles calculated by the two codes at core inlet, middle and outlet core z-planes are compared from Fig. 37 to Fig. 39. The slight discrepancy observed at core inlet (Fig. 37) could be produced by the different turbulence flow modelling implemented in the two codes. Indeed, while the FEM-LCORE implements classical turbulence model for the lower plenum, the pressure distribution calculated by SIMMER-III in that large volume depends mainly on flow mixing and corresponding momentum losses. Both codes predict a more or less uniform pressure profile at core middle z-plane as shown in Fig. 38. The discrepancy observed in Fig. 39 at the core outlet z-plane is mainly related to upper plenum FA supporting structure effect, as clearly demonstrated in section 5.4.

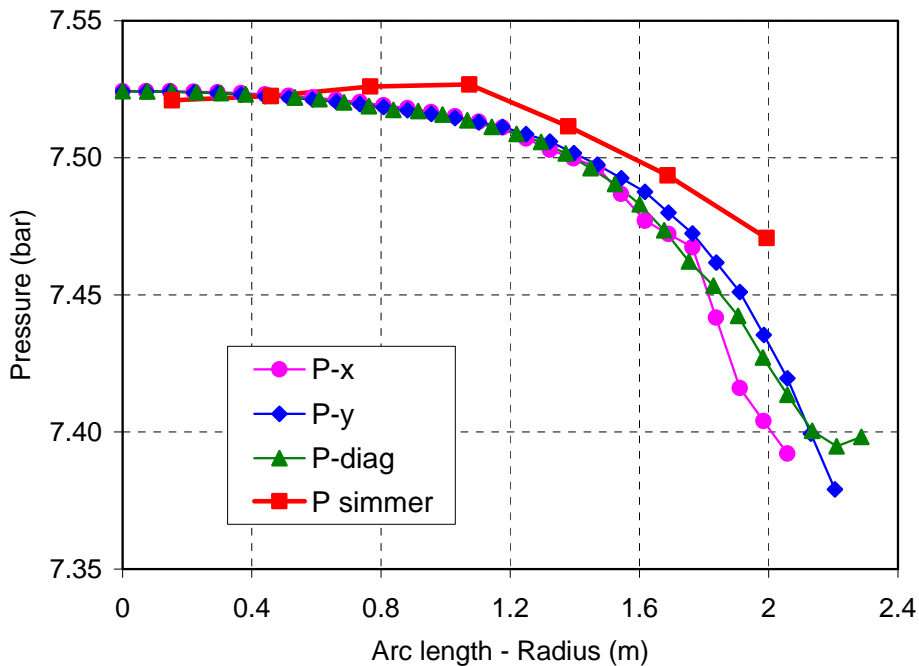


Fig. 37 – Radial pressure profile at core inlet z-plane

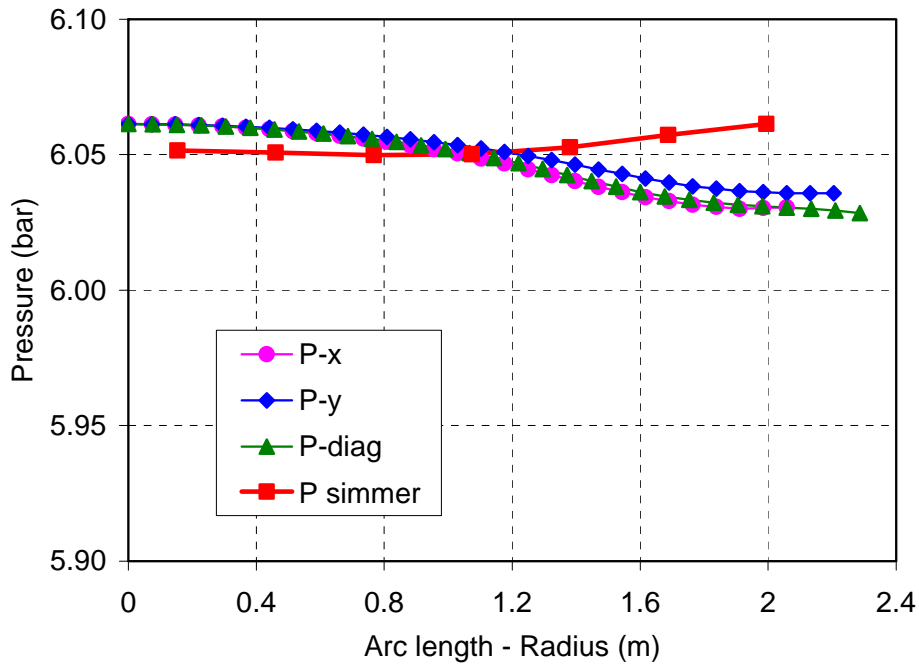


Fig. 38 – Radial pressure profile at core middle z-plane

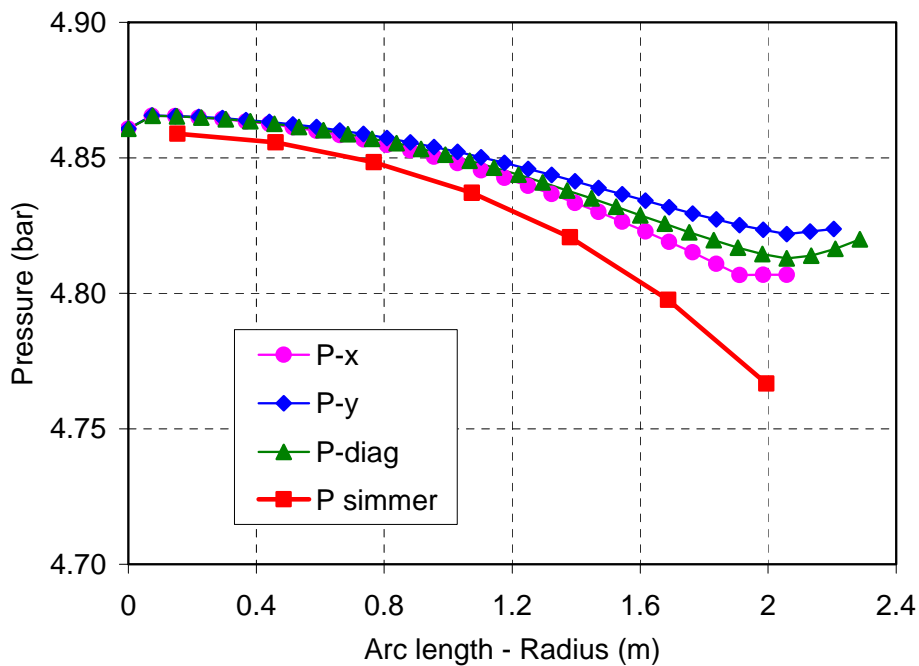


Fig. 39 – Radial pressure profile at core outlet z-plane

## 5.2 Core Lead Velocity

The radial profiles of vertical lead velocity calculated by the two codes at core inlet, middle and outlet core z-planes are compared from Fig. 40 to Fig. 42. The agreement is very good at the core bottom (Fig. 40). Some discrepancy appears towards core periphery at core middle



(Fig. 41), which is consistent with different pressure behaviour at that elevation. Once more, the discrepancies observed at core top (Fig. 42) mainly depend on upper plenum FA supporting structure effect (see section 5.4).

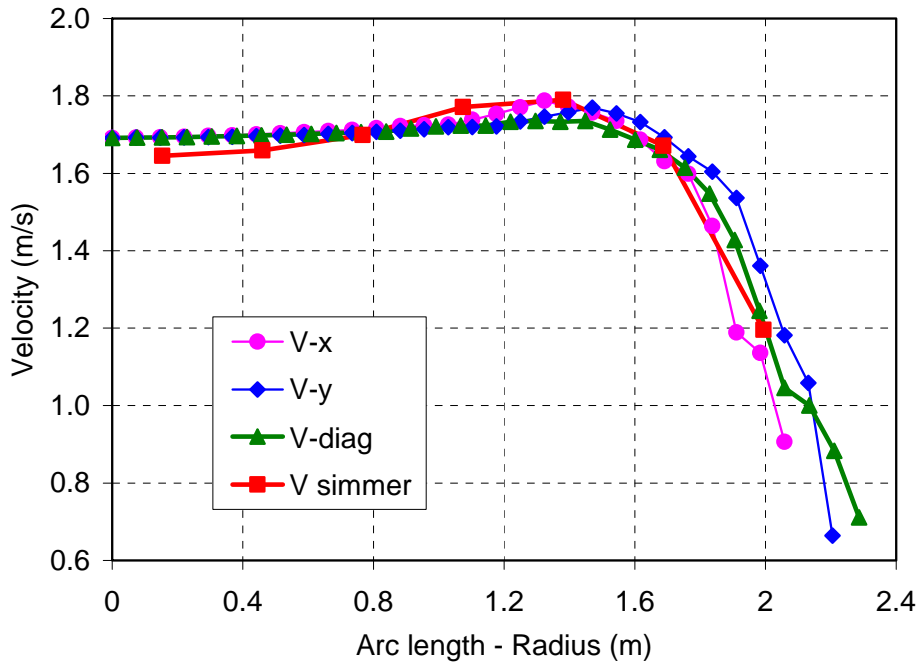


**Fig. 40 – Radial profile of vertical lead velocity at core inlet z-plane**

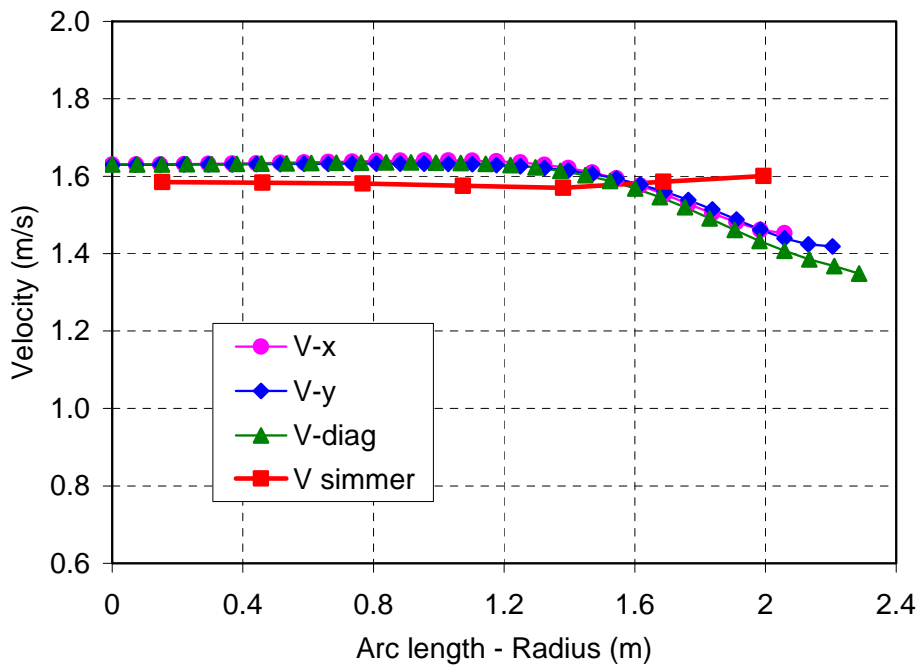


**Fig. 41 – Radial profile of vertical lead velocity at core middle z-plane**

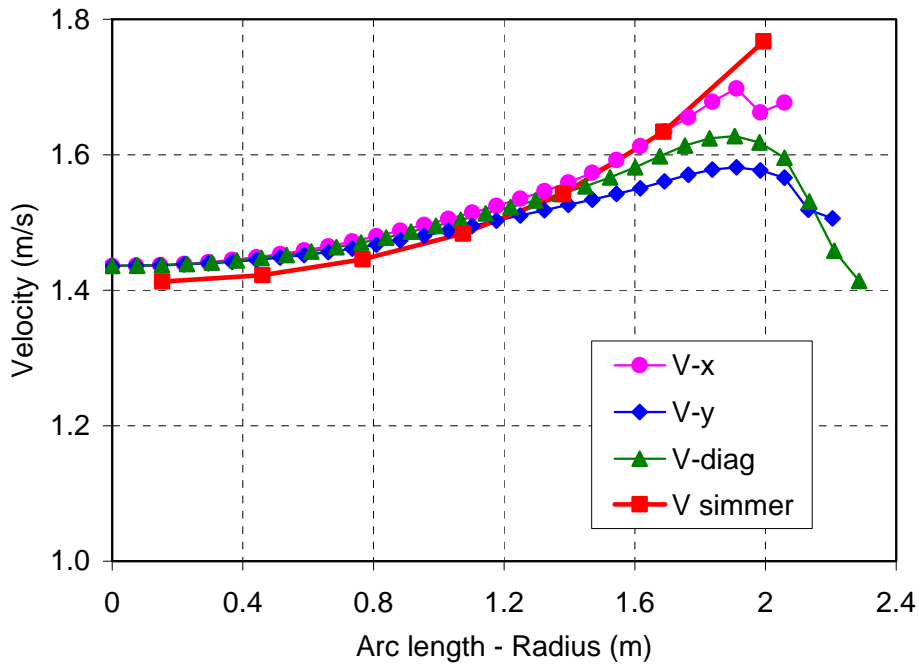


Fig. 42 – Radial profile of vertical lead velocity at core outlet z-plane

### 5.3 Core Lead Temperatures

The radial profile of lead temperature at core top calculated by the two codes is compared in Fig. 43, while the axial temperature profile in the hot spot zone ( $R_c = 1.7$  m or radial mesh 6 in SIMMER-III domain) is shown in Fig. 44.

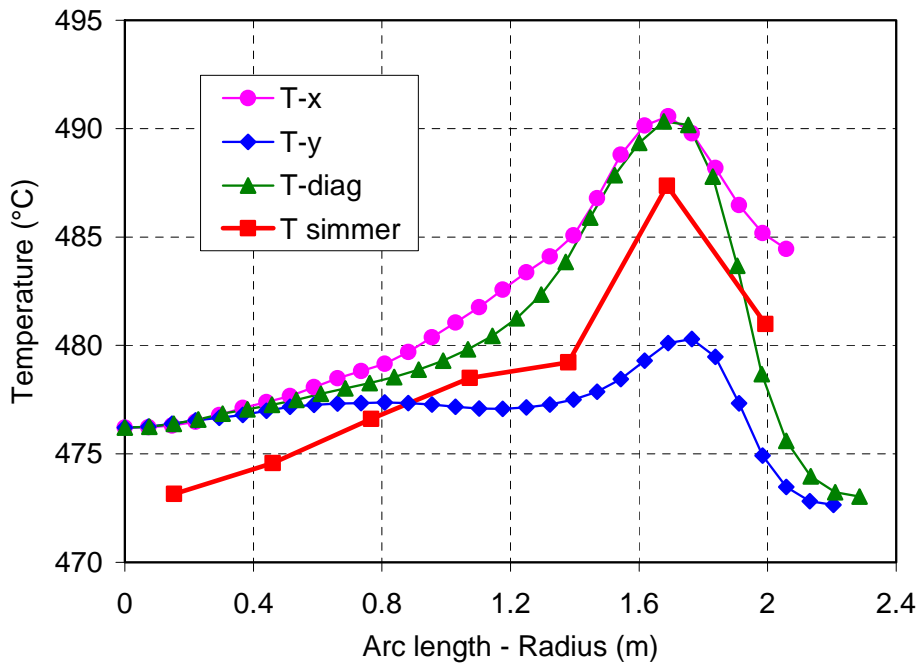
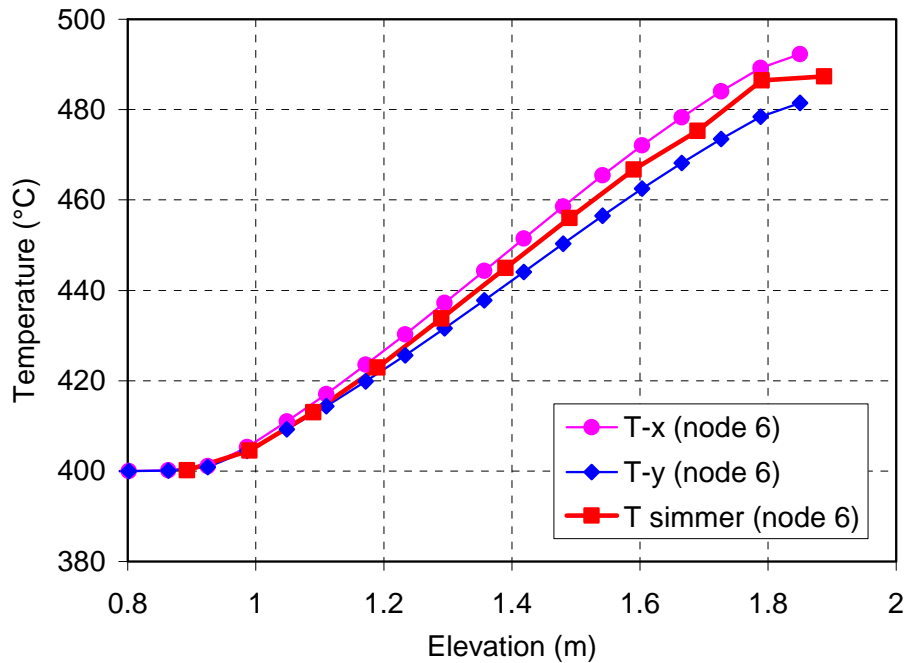


Fig. 43 – Radial profile of lead temperature at core outlet z-plane



**Fig. 44 – Axial profile of lead temperature in the active core at  $R_c = 1.7$  m**

The radial power factor in the 2D SIMMER-III simulation is made consistent with the FA power distribution along the x-axis of the 3D FEM-LCORE model, in order to put in evidence the hot spot with the 2D model. However, because of the homogenization along the circumference, the radial profile calculated by SIMMER-III is clearly shifted about 3 to 5 °C below the corresponding x-axis FEM-LCORE profile, otherwise the average lead  $\Delta T$  over the core (80 °C) would be significantly overestimated by the 2D model. The axial temperature profile calculated by SIMMER-III well compare with the FEM-LCORE ones (see Fig. 44).

As expected, the simplification introduced in the core power distribution with the 2D model leads to underestimate the hot spots with respect to a more detailed 3D model. However, also thanks to the general good agreement of lead flow redistribution within the open core, the under prediction of maximum lead temperature at core outlet by the 2D model is limited to approximately 5 °C.

## 5.4 Influence of Upper Plenum FA Supporting Structures

The influence of upper plenum FA supporting structures on flow and temperature redistribution at the core outlet has been investigated by removing these structures in the 2D SIMMER-III model.

From 45 to Fig. 47, the results of the new 2D calculation regarding radial profiles at core top are compared with the ones described in the previous section 4. The absence of upper plenum FA supporting structures (ups) in the 2D model results in reduced pressure gradient at the core outlet in better agreement with the 3D results (see Fig. 45). Also the new lead velocity profile at core top shown in Fig. 46 tends to best approximate the corresponding profiles calculated by the 3D model in the different directions.

In spite of the substantial deviations observed in velocity profile at the core outlet without upper plenum FA supporting structures, the radial temperature profile and maximum lead temperature at core top calculated by SIMMER-III code are not significantly affected (see Fig. 47).

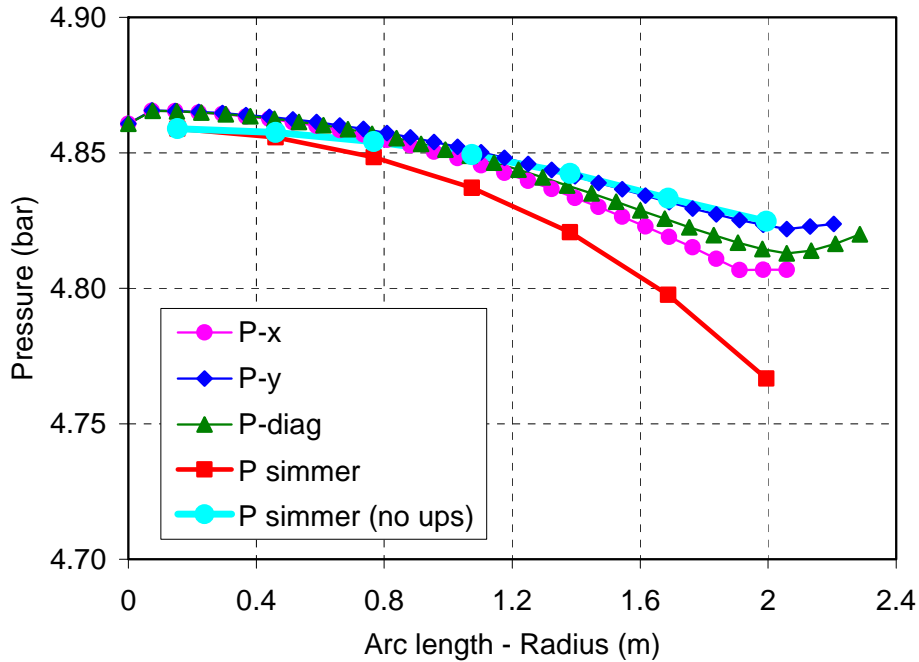


**Fig. 45 – Radial pressure profile at core outlet z-plane**  
(No FA supporting structures)

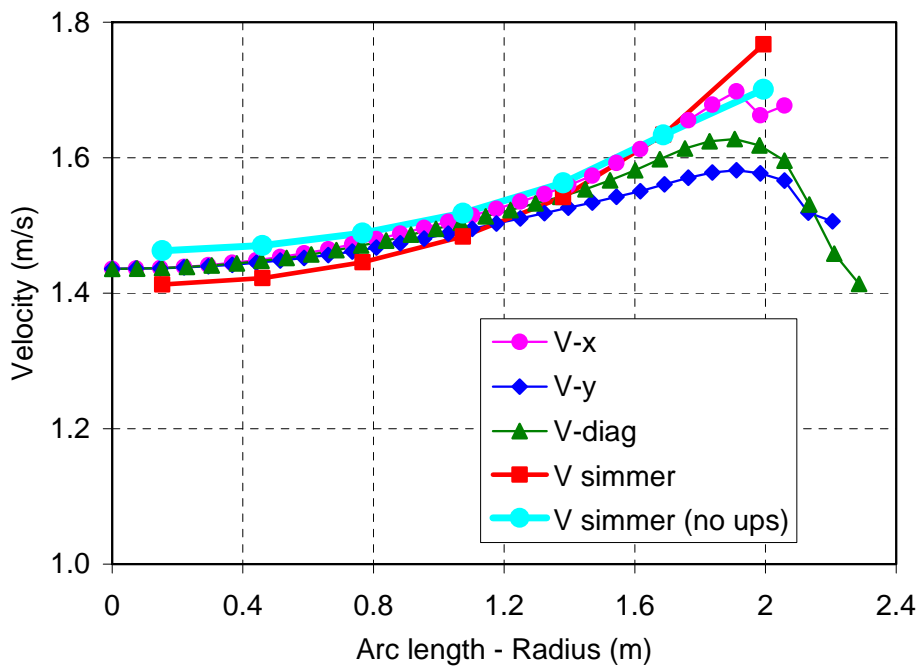


**Fig. 46 – Radial profile of vertical velocity at core outlet z-plane**  
(No FA supporting structures)

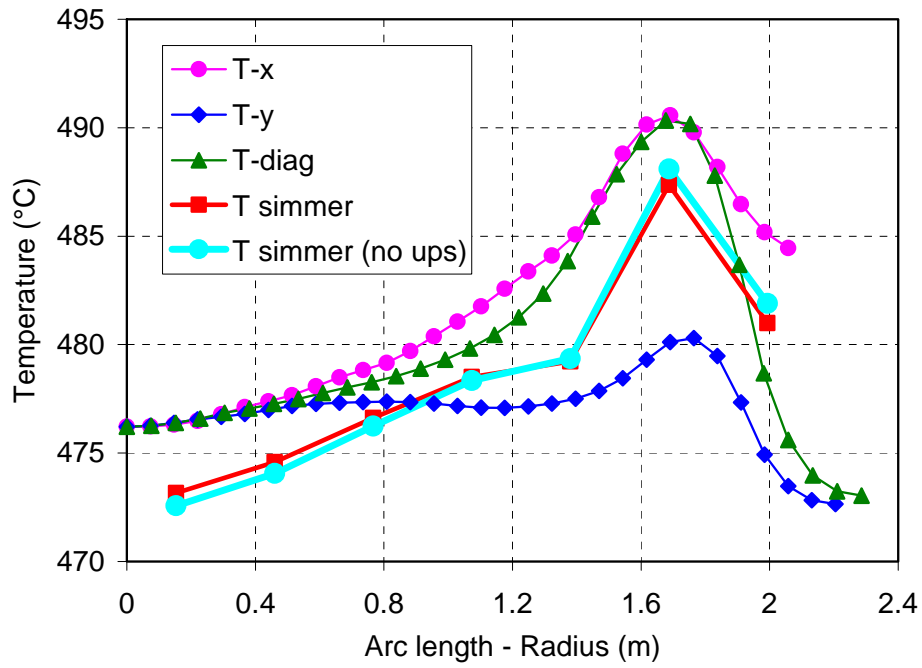


**Fig. 47 – Radial profile of lead temperature at core outlet z-plane**  
(No FA supporting structures)

 <b>Ricerca Sistema Elettrico</b>	<b>Sigla di identificazione</b>	<b>Rev.</b>	<b>Distrib.</b>	<b>Pag.</b>	<b>di</b>
	NNFISS – LP3 - 001	0	L	36	58

## 6. CONCLUSIONS

The present work, written in the framework of the national ENEA-MSE program, is a preliminary attempt to validate a 3D CFD model of the lead-cooled ELSY reactor developed jointly with the University of Bologna. In this report we compare the results obtained with the 3D FEM-LCORE and 2D SIMMER-III code which has been developed and validated worldwide for thermo-fluid dynamic analysis of liquid metal fast reactors.

In spite of the less detailed 2D SIMMER-III simulation with respect to the three-dimensional calculation performed with the FEM-LCORE model, the SIMMER-III results constitute an important reference point for the assessment of the global response of the CFD code. Furthermore, the SIMMER-III analysis, involving the whole primary system of the ELSY reactor, has provided the conditions at the boundary of the CFD model calculation domain.


The broad comparison of pressure, velocity and temperature distribution in the different core regions has highlighted a general good agreement between the two code results, in particular regarding the influence of turbulent phenomena in lower and upper plenum on cross-flows and consequent flow redistribution within the open square ELSY core. A sensitive analysis with SIMMER-III has demonstrated that the largest discrepancies in pressure and velocity radial profiles observed at the core outlet can be correlated to the lack of an upper plenum FA supporting structure model in the CDF code. Furthermore, the code benchmark has demonstrated how the greater accuracy of the 3D FEM-LCORE model can put in evidence eventual non-homogeneities and hot spots in the core that, of course, are not calculated in the 2D approximation with the SIMMER-III code.

Finally, the activity performed in this framework in close cooperation with the University of Bologna has contributed significantly to confirm the capabilities and suitability of FEM-LCORE code, in view of its more generalized use for the assessment of thermo-fluid dynamic behaviour of innovative nuclear reactors.

 <b>Ricerca Sistema Elettrico</b>	<b>Sigla di identificazione</b>	<b>Rev.</b>	<b>Distrib.</b>	<b>Pag.</b>	<b>di</b>
	NNFISS – LP3 - 001	0	L	37	58

## 7. REFERENCES

- 1 L. Cinotti et al., “The potential of the LFR and the ELSY Project”, Proc. of 2007 International Congress on Advances in Nuclear Power Plants (ICAPP '07), Nice, France, May 13-18, 2007 (2007).
- 2 C. Artioli, G. Grasso, M. Sarotto and J. Krepel, “ELSY Neutronic Analysis by deterministic and Monte Carlo methods: an innovative concept for the control rod systems,” Proc. of 2009 International Congress on Advances in Nuclear Power Plants (ICAPP '09), Tokyo, Japan, May 10-14, 2009 (2009).
- 3 N. Yamano et al., “SIMMER-III: A Computer Program for LMFR Core Disruptive Accident Analysis”, Research Document, O-Arai Engineering Center, Japan Nuclear Cycle Development Institute, JNC TN9400 2003-071.
- 4 Y. Tobita et al., “The Development of SIMMER-III, An Advanced Computer Program for LMFR Safety Analysis”, Joint IAEA/NEA Technical Meeting on the Use of Computational Fluid Dynamic Code for Safety Analysis of Reactor Systems, Including Containment, Pisa, Italy, November 2002.
- 5 Cervone and S. Manservigi, “A Three-Dimensional CFD Program for the Simulation of the Thermal-Hydraulic Behavior of an Open Core Liquid Metal Reactor”, Technical Report LIN-THRG 108, XUNIBO-P9LU-001, December 2008.
- 6 S. Bna, S. Manservigi and O. Le Bot, “Simulation of the Thermo-Hydraulic Behaviour of Liquid Metal Reactors Using a Three-Dimensional Finite Element Model”, Univ. of Bologna Technical Report LIN-THRG 110, September 2010.

 <b>Ricerca Sistema Elettrico</b>	<b>Sigla di identificazione</b>	<b>Rev.</b>	<b>Distrib.</b>	<b>Pag.</b>	<b>di</b>
	NNFISS – LP3 - 001	0	L	38	58

## Appendix A: SIMMER-III Input Deck

START : ELSY - Forced Circulation - 2D - Steady-State at Nominal Power

&XCNTL

EDTOPT(6)=1,1,  
ALGOPT(3)=1,  
ALGOPT(59)=1,  
MXFOPT(3)=1,  
MXFOPT(95)=1,

/

\*\*\*\*\*  
\*\*\*  
\*\*\* RZ Cylindrical geometry (radial and axial meshing)  
\*\*\*  
\*\*\*\*\*

&XMSH

IGEOM=0,  
IB=27,JB=61,  
DRINP(1)=7\*0.30675,2\*0.228,2\*0.185875,3\*0.15707,6\*0.20335,  
7\*0.21196,  
DZINP(1)=13\*0.1,10\*0.095,9\*0.1,0.095,12\*0.103333,0.12,0.17,  
0.21,10\*0.2644,0.17,0.50,1.0,  
NREG=44,  
ICL=1,  
ICR=27,  
JCB=1,  
JCT=61,

/

\*\*\*\*\*  
\*\*\*  
\*\*\* Equations of State (EOS)  
\*\*\*  
\*\*\*\*\*

&XEOS

TGMIN=100.D0,  
  
ESOLUS(3,3) = 8.56860D+04,  
ELIQUS(3,3) = 8.56860D+04,  
  
ISAE(2,5) = 0,  
IMRK(2,5) = 0,  
TLIQUS(2,5) = 2.17700E+00,  
TCRT(2,5) = 5.20000E+00,  
ELIQGD(2,5) = -9.27579E+04,  
CVG(2,5) = 3.13400E+02,  
RUGM(2,5) = 4.81447E+02,  
WM(2,5) = 4.00300E+00,

VSOLUS(2,1) = 1.0D-19,  
VSOLUS(2,2) = 1.0D-9,

/



```
*****  
***  
*** Thermo-physical properties of materials  
***  
*****
```

```
&XTPP
```

```
KPOPT(2,5) = 0,  
MUOPT(2,5) = 0,  
EPSM(2,5) = 1.02200E+01,  
SIGM(2,5) = 2.55100E+00,  
NATOM(2,5) = 1,  
/  
/
```

```
*****  
***  
*** Transient time and time-step  
***  
*****
```

```
&XTME
```

```
TWFIN=200.,DTSTRT=1.D-05,DTMIN=1.D-08,DTMAX=3.3D-02,  
TCPU=10000000.,  
/  
/
```

```
*****  
***  
*** Definition of ELSY primary system  
***  
*****
```

```
&XRGN
```

```
RGNAMB=' LEAD_T673 ',  
LRGN=1, ILB=1,IUB=27,JLB=1,JUB=61,  
ALMINB(3) = 1.0,  
TLMINB(3) = 673., TGINB = 673.,  
PSFINB = 2.0D5,  
/  
/
```

```
&XRGN
```

```
RGNAMB=' COVER GAS ',  
LRGN=2, ILB=1,IUB=27,JLB=60,JUB=61,  
TGINB = 673.,  
PSFINB = 1.105D5,  
PG4INB = 1.105D5,  
/  
/
```

```
&XRGN
```

```
RGNAMB=' WALL1 ',  
LRGN=3, ILB=10,IUB=11,JLB=44,JUB=61,  
TGINB = 673.,  
PSFINB = 1.0D5,  
PG4INB = 1.0D5,  
NST1B=1,  
/  
/
```

```
&XRGN
```

```
RGNAMB=' WALL2 ',
```

```
LRGN=4, ILB=10,IUB=11,JLB=14,JUB=35,  
TGINB = 673.,  
PSFINB = 1.0D5,  
PG4INB = 1.0D5,  
NST1B=1,  
/  

```

```
&XRGN
```

```
RGNAMB= ' WALL3 ',  
LRGN=5, ILB=12,IUB=12,JLB=36,JUB=36,  
TGINB = 673.,  
PSFINB = 1.0D5,  
PG4INB = 1.0D5,  
NST1B=1,  
/  

```

```
&XRGN
```

```
RGNAMB= ' WALL4 ',  
LRGN=6, ILB=13,IUB=13,JLB=37,JUB=37,  
TGINB = 673.,  
PSFINB = 1.0D5,  
PG4INB = 1.0D5,  
NST1B=1,  
/  

```

```
&XRGN
```

```
RGNAMB= ' WALL5 ',  
LRGN=7, ILB=14,IUB=14,JLB=38,JUB=38,  
TGINB = 673.,  
PSFINB = 1.0D5,  
PG4INB = 1.0D5,  
NST1B=1,  
/  

```

```
&XRGN
```

```
RGNAMB= ' WALL6 ',  
LRGN=8, ILB=15,IUB=15,JLB=39,JUB=47,  
TGINB = 673.,  
PSFINB = 1.0D5,  
PG4INB = 1.0D5,  
NST1B=1,  
/  

```

```
&XRGN
```

```
RGNAMB= ' WALL7 ',  
LRGN=9, ILB=15,IUB=20,JLB=48,JUB=48,  
TGINB = 673.,  
PSFINB = 1.0D5,  
PG4INB = 1.0D5,  
NST1B=1,  
/  

```

```
&XRGN
```

```
RGNAMB= ' WALL8 ',  
LRGN=10, ILB=15,IUB=20,JLB=61,JUB=61,  
TGINB = 673.,  
PSFINB = 1.0D5,  
PG4INB = 1.0D5,  
NST1B=1,  

```

/

&amp;XRGN

```
  RGNAMB=' LOWER1 ',
  LRGN=11, ILB=3, IUB=27, JLB=1, JUB=1,
  TGINB = 673.,
  PSFINB = 1.0D5,
  PG4INB = 1.0D5,
  NST1B=1,
```

/

&amp;XRGN

```
  RGNAMB=' LOWER2 ',
  LRGN=12, ILB=5, IUB=27, JLB=2, JUB=2,
  TGINB = 673.,
  PSFINB = 1.0D5,
  PG4INB = 1.0D5,
  NST1B=1,
```

/

&amp;XRGN

```
  RGNAMB=' LOWER3 ',
  LRGN=13, ILB=7, IUB=27, JLB=3, JUB=3,
  TGINB = 673.,
  PSFINB = 1.0D5,
  PG4INB = 1.0D5,
  NST1B=1,
```

/

&amp;XRGN

```
  RGNAMB=' LOWER4 ',
  LRGN=14, ILB=9, IUB=27, JLB=4, JUB=4,
  TGINB = 673.,
  PSFINB = 1.0D5,
  PG4INB = 1.0D5,
  NST1B=1,
```

/

&amp;XRGN

```
  RGNAMB=' LOWER5 ',
  LRGN=15, ILB=10, IUB=27, JLB=5, JUB=5,
  TGINB = 673.,
  PSFINB = 1.0D5,
  PG4INB = 1.0D5,
  NST1B=1,
```

/

&amp;XRGN

```
  RGNAMB=' LOWER6 ',
  LRGN=16, ILB=11, IUB=27, JLB=6, JUB=6,
  TGINB = 673.,
  PSFINB = 1.0D5,
  PG4INB = 1.0D5,
  NST1B=1,
```

/

&amp;XRGN

```
  RGNAMB=' LOWER7 ',
  LRGN=17, ILB=12, IUB=27, JLB=7, JUB=7,
```

```
TGINB = 673.,  
PSFINB = 1.0D5,  
PG4INB = 1.0D5,  
NST1B=1,  
/  

```

```
&XRGN
```

```
  RGNAMB=' LOWER8 ',  
  LRGN=18, ILB=13,IUB=27,JLB=8,JUB=8,  
  TGINB = 673.,  
  PSFINB = 1.0D5,  
  PG4INB = 1.0D5,  
  NST1B=1,  
  /  

```

```
&XRGN
```

```
  RGNAMB=' LOWER9 ',  
  LRGN=19, ILB=14,IUB=27,JLB=9,JUB=9,  
  TGINB = 673.,  
  PSFINB = 1.0D5,  
  PG4INB = 1.0D5,  
  NST1B=1,  
  /  

```

```
&XRGN
```

```
  RGNAMB=' LOWER10 ',  
  LRGN=20, ILB=15,IUB=27,JLB=10,JUB=10,  
  TGINB = 673.,  
  PSFINB = 1.0D5,  
  PG4INB = 1.0D5,  
  NST1B=1,  
  /  

```

```
&XRGN
```

```
  RGNAMB=' LOWER11 ',  
  LRGN=21, ILB=16,IUB=27,JLB=11,JUB=11,  
  TGINB = 673.,  
  PSFINB = 1.0D5,  
  PG4INB = 1.0D5,  
  NST1B=1,  
  /  

```

```
&XRGN
```

```
  RGNAMB=' LOWER12 ',  
  LRGN=22, ILB=17,IUB=27,JLB=12,JUB=13,  
  TGINB = 673.,  
  PSFINB = 1.0D5,  
  PG4INB = 1.0D5,  
  NST1B=1,  
  /  

```

```
&XRGN
```

```
  RGNAMB=' LOWER13 ',  
  LRGN=23, ILB=18,IUB=27,JLB=14,JUB=15,  
  TGINB = 673.,  
  PSFINB = 1.0D5,  
  PG4INB = 1.0D5,  
  NST1B=1,  
  /  

```

&amp;XRGN

```
  RGNAMB=' LOWER14 ',  
  LRGN=24, ILB=19, IUB=27, JLB=16, JUB=17,  
  TGINB = 673.,  
  PSFINB = 1.0D5,  
  PG4INB = 1.0D5,  
  NST1B=1,  
/
```

&amp;XRGN

```
  RGNAMB=' LOWER15 ',  
  LRGN=25, ILB=20, IUB=27, JLB=18, JUB=19,  
  TGINB = 673.,  
  PSFINB = 1.0D5,  
  PG4INB = 1.0D5,  
  NST1B=1,  
/
```

&amp;XRGN

```
  RGNAMB=' LOWER16 ',  
  LRGN=26, ILB=21, IUB=27, JLB=20, JUB=21,  
  TGINB = 673.,  
  PSFINB = 1.0D5,  
  PG4INB = 1.0D5,  
  NST1B=1,  
/
```

&amp;XRGN

```
  RGNAMB=' LOWER17 ',  
  LRGN=27, ILB=22, IUB=27, JLB=22, JUB=23,  
  TGINB = 673.,  
  PSFINB = 1.0D5,  
  PG4INB = 1.0D5,  
  NST1B=1,  
/
```

&amp;XRGN

```
  RGNAMB=' LOWER18 ',  
  LRGN=28, ILB=23, IUB=27, JLB=24, JUB=26,  
  TGINB = 673.,  
  PSFINB = 1.0D5,  
  PG4INB = 1.0D5,  
  NST1B=1,  
/
```

&amp;XRGN

```
  RGNAMB=' LOWER19 ',  
  LRGN=29, ILB=24, IUB=27, JLB=27, JUB=29,  
  TGINB = 673.,  
  PSFINB = 1.0D5,  
  PG4INB = 1.0D5,  
  NST1B=1,  
/
```

&amp;XRGN

```
  RGNAMB=' LOWER20 ',  
  LRGN=30, ILB=25, IUB=27, JLB=30, JUB=32,  
  TGINB = 673.,
```

```
PSFINB = 1.0D5,  
PG4INB = 1.0D5,  
NST1B=1,  
/  

```

```
&XRGN
```

```
  RGNAMB=' LOWER21 ',  
  LRGN=31, ILB=26, IUB=27, JLB=33, JUB=36,  
  TGINB = 673.,  
  PSFINB = 1.0D5,  
  PG4INB = 1.0D5,  
  NST1B=1,  
/  

```

```
&XRGN
```

```
  RGNAMB=' LOWER22 ',  
  LRGN=32, ILB=27, IUB=27, JLB=37, JUB=41,  
  TGINB = 673.,  
  PSFINB = 1.0D5,  
  PG4INB = 1.0D5,  
  NST1B=1,  
/  

```

```
&XRGN
```

```
  RGNAMB=' CORE INLET ',  
  LRGN=33, ILB=1, IUB=7, JLB=13, JUB=13,  
  ALMINB(3) = 0.93,  
  TLMINB(3) = 673., TGINB = 673.,  
  ASMINB(5) = 0.03,  
  ASMINB(6) = 0.005, ALCWIB = 5.0,  
  TSINB(5) = 673., TSINB(6) = 673.,  
  ASMINB(7) = 0.03,  
  ASMINB(8) = 0.005, ARCWIB = 5.0,  
  TSINB(7) = 673., TSINB(8) = 673.,  
  PSFINB = 2.0D5,  
  ILS0IB=7,  
/  

```

```
&XRGN
```

```
  RGNAMB=' CORE ',  
  LRGN=34, ILB=1, IUB=7, JLB=23, JUB=33,  
  ALMINB(3) = 0.518,  
  TLMINB(3) = 673., TGINB = 673.,  
  ASMINB(1) = 0.06454,  
  ASMINB(4) = 0.10385,  
  ANFIPB = 0.02561,  
  ASMTB = 0.288,  
  TSINB(1) = 673.,  
  TSINTB = 673., TSINB(4) = 673.,  
  PSFINB = 2.0D5,  
  RPINIB = 0.00525,  
  XENRIB = 1.,0.,0.,0.,0.,0.,  
  ILS0IB=7,  
/  

```

```
&XRGN
```

```
  RGNAMB=' GAS_PLENUM ',  
  LRGN=35, ILB=1, IUB=7, JLB=14, JUB=22,  
  ALMINB(3) = 0.518,  
/  

```

```
TLMINB(3) = 673., TGINB = 673.,  
ASMINB(1) = 0.0,  
ASMINB(4) = 0.10385,  
ANFIPB = 0.37815,  
ASMTB = 0.0,  
TSINB(1) = 673.,  
TSINTB = 673., TSINB(4) = 673.,  
PSFINB = 2.0D5,  
RPINIB = 0.00525,  
XENRIB = 1.,0.,0.,0.,0.,0.,  
ILS0IB=7,  
/  

```

&XRGN

```
RGNAMB=' REFLECTOR ',  
LRGN=36, ILB=8,IUB=9,JLB=14,JUB=33,  
ALMINB(3) = 0.800,  
TLMINB(3) = 673., TGINB = 673.,  
ASMINB(1) = 0.02,  
ASMINB(4) = 0.03,  
ANFIPB = 0.0,  
ASMTB = 0.08  
TSINB(1) = 673.,  
TSINTB = 673., TSINB(4) = 673.,  
ASMINB(5) = 0.03,  
ASMINB(6) = 0.005, ALCWIB = 5.0,  
TSINB(5) = 673., TSINB(6) = 673.,  
ASMINB(7) = 0.03,  
ASMINB(8) = 0.005, ARCWIB = 5.0,  
TSINB(7) = 673., TSINB(8) = 673.,  
PSFINB = 2.0D5,  
RPINIB = 0.00525,  
XENRIB = 1.,0.,0.,0.,0.,0.,  
ILS0IB=7,  
/  

```

&XRGN

```
RGNAMB=' UPPER_PLENUM ',  
LRGN=37, ILB=1,IUB=9,JLB=34,JUB=45,  
ALMINB(3) = 0.78,  
TLMINB(3) = 673., TGINB = 673.,  
ASMINB(1) = 0.05,  
ASMINB(4) = 0.05,  
ANFIPB = 0.0,  
ASMTB = 0.12,  
TSINB(1) = 673.,  
TSINTB = 673., TSINB(4) = 673.,  
PSFINB = 2.0D5,  
RPINIB = 0.077,  
XENRIB = 1.,0.,0.,0.,0.,0.,  
ILS0IB=7,  
/  

```

&XRGN

```
RGNAMB=' UPPER_HEAD ',  
LRGN=38, ILB=1,IUB=9,JLB=46,JUB=59,  
ALMINB(3) = 0.15,  
TLMINB(3) = 673., TGINB = 673.,  
ASMINB(1) = 0.05,  

```

```
ASMINB(4) = 0.05,  
ANFIPB = 0.0,  
ASMTB = 0.75,  
TSINB(1) = 673.,  
TSINTB = 673., TSINB(4) = 673.,  
PSFINB = 2.0D5,  
RPINIB = 0.140,  
XENRIB = 1.,0.,0.,0.,0.,0.,  
ILS0IB=7,  
/  

```

&XRCN

```
RGNAMB=' UPPER_HEAD1 ',  
LRGN=39, ILB=1,IUB=9,JLB=56,JUB=56,  
ALMINB(3) = 0.05,  
TLMINB(3) = 673., TGINB = 673.,  
ASMINB(1) = 0.10,  
ASMINB(4) = 0.05,  
ANFIPB = 0.0,  
ASMTB = 0.50,  
TSINB(1) = 673.,  
TSINTB = 673., TSINB(4) = 673.,  
PSFINB = 1.107D5,  
RPINIB = 0.140,  
XENRIB = 1.,0.,0.,0.,0.,0.,  
ILS0IB=7,  
/  

```

&XRCN

```
RGNAMB=' HEAD_TOP ',  
LRGN=40, ILB=1,IUB=9,JLB=57,JUB=61,  
ALMINB(3) = 0.0,  
TLMINB(3) = 673., TGINB = 673.,  
ASMINB(1) = 0.05,  
ASMINB(4) = 0.05,  
ANFIPB = 0.0,  
ASMTB = 0.75,  
TSINB(1) = 673.,  
TSINTB = 673., TSINB(4) = 673.,  
PSFINB = 1.10D5,  
RPINIB = 0.140,  
XENRIB = 1.,0.,0.,0.,0.,0.,  
ILS0IB=7,  
/  

```

&XRCN

```
RGNAMB=' STEAM_GEN ',  
LRGN=41, ILB=15,IUB=20,JLB=49,JUB=58,  
ALMINB(3) = 0.477,  
TLMINB(3) = 673., TGINB = 673.,  
ASMINB(1) = 0.10,  
ASMINB(4) = 0.05,  
ANFIPB = 0.0,  
ASMTB = 0.373,  
TSINB(1) = 663.0,  
TSINTB = 663.0, TSINB(4) = 663.0,  
PSFINB = 2.0D5,  
RPINIB = 0.0125,  
XENRIB = 1.,0.,0.,0.,0.,0.,
```



```
ILS0IB=7,  
/
```

```
&XRCN
```

```
  RGNAMB=' STEAM_GTOP1 ',  
  LRGN=42, ILB=15,IUB=20,JLB=59,JUB=59,  
  ALMINB(3) = 0.15,  
  TLMINB(3) = 673., TGINB = 673.,  
  ASMINB(1) = 0.15,  
  ASMINB(4) = 0.10,  
  ANFIPB = 0.0,  
  ASMTB = 0.60,  
  TSINB(1) = 673.,  
  TSINTB = 673., TSINB(4) = 673.,  
  PSFINB = 1.20D5,  
  RPINIB = 0.0125,  
  XENRIB = 1.,0.,0.,0.,0.,0.,  
  ILS0IB=7,  
/
```

```
&XRCN
```

```
  RGNAMB=' STEAM_GTOP2 ',  
  LRGN=43, ILB=15,IUB=20,JLB=60,JUB=60,  
  ALMINB(3) = 0.0,  
  TLMINB(3) = 673., TGINB = 673.,  
  ASMINB(1) = 0.15,  
  ASMINB(4) = 0.10,  
  ANFIPB = 0.0,  
  ASMTB = 0.60,  
  TSINB(1) = 673.,  
  TSINTB = 673., TSINB(4) = 673.,  
  PSFINB = 1.10D5,  
  RPINIB = 0.0125,  
  XENRIB = 1.,0.,0.,0.,0.,0.,  
  ILS0IB=7,  
/
```

```
&XRCN
```

```
  RGNAMB=' LEAD_PUMP ',  
  LRGN=44, ILB=12,IUB=14,JLB=60,JUB=60,  
  ALMINB(3) = 1.0,  
  TLMINB(3) = 673., TGINB = 673.,  
  PSFINB = 2.0D5,  
/
```

```
*****  
***  
***  Boundary conditions and pump model  
***  
*****
```

```
&XBND
```

```
  NBC=0,  
  LBCSET(1)=    29*0,  
                1769*0,  
                29*0,  
  
  LVPSET(1)=    29*0,  
                1334*0,
```

```
12*0,1,1,1,14*0,  
406*0,  
29*0,  
LVPMP(1)=9,  
VPMTAB(1,1)=1.650E5,1.65E5,1.650E4,7.32E3,3.42E3,1.55E3,5.77E2,  
0.0,0.0,  
VPMTME(1,1)=0.,200.,201.,202.,203.,205.,210.,  
220.,10000.,
```

```
LWASET(15,50)=0011,  
LWASET(15,52)=0011,  
LWASET(15,54)=0011,  
LWASET(15,56)=0011,  
LWASET(15,58)=0011,
```

```
LWASET(20,50)=0011,  
LWASET(20,52)=0011,  
LWASET(20,54)=0011,  
LWASET(20,56)=0011,  
LWASET(20,58)=0011,
```

/

&XBND

```
NBC=1,LBCS=2,LBCP=2,LBCG=1,  
PTME(1)=0.0,10000.0,  
PTAB(1)=1.10E5,1.10E5,
```

/

```
*****  
***  
*** Singular pressure loss coefficients  
***  
*****
```

&XMXF

```
CORFZN(1,14)=0.159,  
CORFZN(2,14)=0.159,  
CORFZN(3,14)=0.159,  
CORFZN(4,14)=0.159,  
CORFZN(5,14)=0.159,  
CORFZN(6,14)=0.159,  
CORFZN(7,14)=0.159,
```

```
CORFZN(1,16)=0.159,  
CORFZN(2,16)=0.159,  
CORFZN(3,16)=0.159,  
CORFZN(4,16)=0.159,  
CORFZN(5,16)=0.159,  
CORFZN(6,16)=0.159,  
CORFZN(7,16)=0.159,
```

```
CORFZN(1,19)=0.159,  
CORFZN(2,19)=0.159,  
CORFZN(3,19)=0.159,  
CORFZN(4,19)=0.159,  
CORFZN(5,19)=0.159,  
CORFZN(6,19)=0.159,  
CORFZN(7,19)=0.159,
```

CORFZN(1,22)=0.159,  
CORFZN(2,22)=0.159,  
CORFZN(3,22)=0.159,  
CORFZN(4,22)=0.159,  
CORFZN(5,22)=0.159,  
CORFZN(6,22)=0.159,  
CORFZN(7,22)=0.159,

CORFZN(1,25)=0.159,  
CORFZN(2,25)=0.159,  
CORFZN(3,25)=0.159,  
CORFZN(4,25)=0.159,  
CORFZN(5,25)=0.159,  
CORFZN(6,25)=0.159,  
CORFZN(7,25)=0.159,

CORFZN(1,28)=0.159,  
CORFZN(2,28)=0.159,  
CORFZN(3,28)=0.159,  
CORFZN(4,28)=0.159,  
CORFZN(5,28)=0.159,  
CORFZN(6,28)=0.159,  
CORFZN(7,28)=0.159,

CORFZN(1,31)=0.159,  
CORFZN(2,31)=0.159,  
CORFZN(3,31)=0.159,  
CORFZN(4,31)=0.159,  
CORFZN(5,31)=0.159,  
CORFZN(6,31)=0.159,  
CORFZN(7,31)=0.159,

CORFZN(1,33)=0.159,  
CORFZN(2,33)=0.159,  
CORFZN(3,33)=0.159,  
CORFZN(4,33)=0.159,  
CORFZN(5,33)=0.159,  
CORFZN(6,33)=0.159,  
CORFZN(7,33)=0.159,

CORFZN(8,14)=4600.,  
CORFZN(9,14)=4600.,  
CORFZN(8,33)=10.,  
CORFZN(9,33)=10.,

CORFZN(12,47)=0.0,  
CORFZN(13,47)=0.0,  
CORFZN(14,47)=0.0,

CORFZN(15,49)=16.2,  
CORFZN(16,49)=16.2,  
CORFZN(17,49)=16.2,  
CORFZN(18,49)=16.2,  
CORFZN(19,49)=16.2,  
CORFZN(20,49)=16.2,

CORFZN(15,50)=16.2,  
CORFZN(16,50)=16.2,  
CORFZN(17,50)=16.2,

CORFZN(18,50)=16.2,  
CORFZN(19,50)=16.2,  
CORFZN(20,50)=16.2,

CORFZN(15,51)=16.2,  
CORFZN(16,51)=16.2,  
CORFZN(17,51)=16.2,  
CORFZN(18,51)=16.2,  
CORFZN(19,51)=16.2,  
CORFZN(20,51)=16.2,

CORFZN(15,52)=16.2,  
CORFZN(16,52)=16.2,  
CORFZN(17,52)=16.2,  
CORFZN(18,52)=16.2,  
CORFZN(19,52)=16.2,  
CORFZN(20,52)=16.2,

CORFZN(15,53)=16.2,  
CORFZN(16,53)=16.2,  
CORFZN(17,53)=16.2,  
CORFZN(18,53)=16.2,  
CORFZN(19,53)=16.2,  
CORFZN(20,53)=16.2,

CORFZN(15,54)=16.2,  
CORFZN(16,54)=16.2,  
CORFZN(17,54)=16.2,  
CORFZN(18,54)=16.2,  
CORFZN(19,54)=16.2,  
CORFZN(20,54)=16.2,

CORFZN(15,55)=16.2,  
CORFZN(16,55)=16.2,  
CORFZN(17,55)=16.2,  
CORFZN(18,55)=16.2,  
CORFZN(19,55)=16.2,  
CORFZN(20,55)=16.2,

CORFZN(15,56)=16.2,  
CORFZN(16,56)=16.2,  
CORFZN(17,56)=16.2,  
CORFZN(18,56)=16.2,  
CORFZN(19,56)=16.2,  
CORFZN(20,56)=16.2,

CORFZN(15,57)=16.2,  
CORFZN(16,57)=16.2,  
CORFZN(17,57)=16.2,  
CORFZN(18,57)=16.2,  
CORFZN(19,57)=16.2,  
CORFZN(20,57)=16.2,

CORFZN(15,58)=1.e3,  
CORFZN(16,58)=1.e3,  
CORFZN(17,58)=1.e3,  
CORFZN(18,58)=1.e3,  
CORFZN(19,58)=1.e3,  
CORFZN(20,58)=1.e3,

CORFZN(15,59)=1.e3,  
CORFZN(16,59)=1.e3,  
CORFZN(17,59)=1.e3,  
CORFZN(18,59)=1.e3,  
CORFZN(19,59)=1.e3,  
CORFZN(20,59)=1.e3,

CORFRN(14,49)=16.2,  
CORFRN(14,50)=16.2,  
CORFRN(14,51)=16.2,  
CORFRN(14,52)=16.2,  
CORFRN(14,53)=16.2,  
CORFRN(14,54)=16.2,  
CORFRN(14,55)=16.2,  
CORFRN(14,56)=16.2,  
CORFRN(14,57)=16.2,  
CORFRN(14,58)=16.2,

CORFRN(15,49)=16.2,  
CORFRN(15,50)=16.2,  
CORFRN(15,51)=16.2,  
CORFRN(15,52)=16.2,  
CORFRN(15,53)=16.2,  
CORFRN(15,54)=16.2,  
CORFRN(15,55)=16.2,  
CORFRN(15,56)=16.2,  
CORFRN(15,57)=16.2,  
CORFRN(15,58)=16.2,

CORFRN(16,49)=16.2,  
CORFRN(16,50)=16.2,  
CORFRN(16,51)=16.2,  
CORFRN(16,52)=16.2,  
CORFRN(16,53)=16.2,  
CORFRN(16,54)=16.2,  
CORFRN(16,55)=16.2,  
CORFRN(16,56)=16.2,  
CORFRN(16,57)=16.2,  
CORFRN(16,58)=16.2,

CORFRN(17,49)=16.2,  
CORFRN(17,50)=16.2,  
CORFRN(17,51)=16.2,  
CORFRN(17,52)=16.2,  
CORFRN(17,53)=16.2,  
CORFRN(17,54)=16.2,  
CORFRN(17,55)=16.2,  
CORFRN(17,56)=16.2,  
CORFRN(17,57)=16.2,  
CORFRN(17,58)=16.2,

CORFRN(18,49)=16.2,  
CORFRN(18,50)=16.2,  
CORFRN(18,51)=16.2,  
CORFRN(18,52)=16.2,  
CORFRN(18,53)=16.2,  
CORFRN(18,54)=16.2,  
CORFRN(18,55)=16.2,

CORFRN(18,56)=16.2,  
CORFRN(18,57)=16.2,  
CORFRN(18,58)=16.2,

CORFRN(19,49)=16.2,  
CORFRN(19,50)=16.2,  
CORFRN(19,51)=16.2,  
CORFRN(19,52)=16.2,  
CORFRN(19,53)=16.2,  
CORFRN(19,54)=16.2,  
CORFRN(19,55)=16.2,  
CORFRN(19,56)=16.2,  
CORFRN(19,57)=16.2,  
CORFRN(19,58)=16.2,

CORFRN(20,49)=16.2,  
CORFRN(20,50)=16.2,  
CORFRN(20,51)=16.2,  
CORFRN(20,52)=16.2,  
CORFRN(20,53)=16.2,  
CORFRN(20,54)=16.2,  
CORFRN(20,55)=16.2,  
CORFRN(20,56)=16.2,  
CORFRN(20,57)=16.2,  
CORFRN(20,58)=16.2,

CORFRN(15,59)=1.0e3,  
CORFRN(16,59)=1.0e3,  
CORFRN(17,59)=1.0e3,  
CORFRN(18,59)=1.0e3,  
CORFRN(19,59)=1.0e3,  
CORFRN(20,59)=1.0e3,

CORFRN(15,60)=1.0e3,  
CORFRN(16,60)=1.0e3,  
CORFRN(17,60)=1.0e3,  
CORFRN(18,60)=1.0e3,  
CORFRN(19,60)=1.0e3,  
CORFRN(20,60)=1.0e3,

CORFZN(1,45)=1.0e5,  
CORFZN(2,45)=1.0e5,  
CORFZN(3,45)=1.0e5,  
CORFZN(4,45)=1.0e5,  
CORFZN(5,45)=1.0e5,  
CORFZN(6,45)=1.0e5,  
CORFZN(7,45)=1.0e5,  
CORFZN(8,45)=1.0e5,  
CORFZN(9,45)=1.0e5,

CORFZN(1,46)=1.0e3,  
CORFZN(2,46)=1.0e3,  
CORFZN(3,46)=1.0e3,  
CORFZN(4,46)=1.0e3,  
CORFZN(5,46)=1.0e3,  
CORFZN(6,46)=1.0e3,  
CORFZN(7,46)=1.0e3,  
CORFZN(8,46)=1.0e3,  
CORFZN(9,46)=1.0e3,

CORFZN(1,47)=1.0e3,  
CORFZN(2,47)=1.0e3,  
CORFZN(3,47)=1.0e3,  
CORFZN(4,47)=1.0e3,  
CORFZN(5,47)=1.0e3,  
CORFZN(6,47)=1.0e3,  
CORFZN(7,47)=1.0e3,  
CORFZN(8,47)=1.0e3,  
CORFZN(9,47)=1.0e3,

CORFZN(1,48)=1.0e3,  
CORFZN(2,48)=1.0e3,  
CORFZN(3,48)=1.0e3,  
CORFZN(4,48)=1.0e3,  
CORFZN(5,48)=1.0e3,  
CORFZN(6,48)=1.0e3,  
CORFZN(7,48)=1.0e3,  
CORFZN(8,48)=1.0e3,  
CORFZN(9,48)=1.0e3,

CORFZN(1,49)=1.0e3,  
CORFZN(2,49)=1.0e3,  
CORFZN(3,49)=1.0e3,  
CORFZN(4,49)=1.0e3,  
CORFZN(5,49)=1.0e3,  
CORFZN(6,49)=1.0e3,  
CORFZN(7,49)=1.0e3,  
CORFZN(8,49)=1.0e3,  
CORFZN(9,49)=1.0e3,

CORFZN(1,50)=1.0e3,  
CORFZN(2,50)=1.0e3,  
CORFZN(3,50)=1.0e3,  
CORFZN(4,50)=1.0e3,  
CORFZN(5,50)=1.0e3,  
CORFZN(6,50)=1.0e3,  
CORFZN(7,50)=1.0e3,  
CORFZN(8,50)=1.0e3,  
CORFZN(9,50)=1.0e3,

CORFZN(1,51)=1.0e3,  
CORFZN(2,51)=1.0e3,  
CORFZN(3,51)=1.0e3,  
CORFZN(4,51)=1.0e3,  
CORFZN(5,51)=1.0e3,  
CORFZN(6,51)=1.0e3,  
CORFZN(7,51)=1.0e3,  
CORFZN(8,51)=1.0e3,  
CORFZN(9,51)=1.0e3,

CORFZN(1,52)=1.0e3,  
CORFZN(2,52)=1.0e3,  
CORFZN(3,52)=1.0e3,  
CORFZN(4,52)=1.0e3,  
CORFZN(5,52)=1.0e3,  
CORFZN(6,52)=1.0e3,  
CORFZN(7,52)=1.0e3,  
CORFZN(8,52)=1.0e3,

CORFZN(9,52)=1.0e3,

CORFZN(1,53)=1.0e3,  
CORFZN(2,53)=1.0e3,  
CORFZN(3,53)=1.0e3,  
CORFZN(4,53)=1.0e3,  
CORFZN(5,53)=1.0e3,  
CORFZN(6,53)=1.0e3,  
CORFZN(7,53)=1.0e3,  
CORFZN(8,53)=1.0e3,  
CORFZN(9,53)=1.0e3,

CORFZN(1,54)=1.0e3,  
CORFZN(2,54)=1.0e3,  
CORFZN(3,54)=1.0e3,  
CORFZN(4,54)=1.0e3,  
CORFZN(5,54)=1.0e3,  
CORFZN(6,54)=1.0e3,  
CORFZN(7,54)=1.0e3,  
CORFZN(8,54)=1.0e3,  
CORFZN(9,54)=1.0e3,

CORFZN(1,55)=1.0e3,  
CORFZN(2,55)=1.0e3,  
CORFZN(3,55)=1.0e3,  
CORFZN(4,55)=1.0e3,  
CORFZN(5,55)=1.0e3,  
CORFZN(6,55)=1.0e3,  
CORFZN(7,55)=1.0e3,  
CORFZN(8,55)=1.0e3,  
CORFZN(9,55)=1.0e3,

CORFZN(1,56)=1.0e3,  
CORFZN(2,56)=1.0e3,  
CORFZN(3,56)=1.0e3,  
CORFZN(4,56)=1.0e3,  
CORFZN(5,56)=1.0e3,  
CORFZN(6,56)=1.0e3,  
CORFZN(7,56)=1.0e3,  
CORFZN(8,56)=1.0e3,  
CORFZN(9,56)=1.0e3,

CORFZN(1,57)=1.0e3,  
CORFZN(2,57)=1.0e3,  
CORFZN(3,57)=1.0e3,  
CORFZN(4,57)=1.0e3,  
CORFZN(5,57)=1.0e3,  
CORFZN(6,57)=1.0e3,  
CORFZN(7,57)=1.0e3,  
CORFZN(8,57)=1.0e3,  
CORFZN(9,57)=1.0e3,

CORFZN(1,58)=1.0e3,  
CORFZN(2,58)=1.0e3,  
CORFZN(3,58)=1.0e3,  
CORFZN(4,58)=1.0e3,  
CORFZN(5,58)=1.0e3,  
CORFZN(6,58)=1.0e3,  
CORFZN(7,58)=1.0e3,



CORFZN(8,58)=1.0e3,  
CORFZN(9,58)=1.0e3,

CORFZN(1,59)=1.0e3,  
CORFZN(2,59)=1.0e3,  
CORFZN(3,59)=1.0e3,  
CORFZN(4,59)=1.0e3,  
CORFZN(5,59)=1.0e3,  
CORFZN(6,59)=1.0e3,  
CORFZN(7,59)=1.0e3,  
CORFZN(8,59)=1.0e3,  
CORFZN(9,59)=1.0e3,

CORFZN(1,60)=1.0e3,  
CORFZN(2,60)=1.0e3,  
CORFZN(3,60)=1.0e3,  
CORFZN(4,60)=1.0e3,  
CORFZN(5,60)=1.0e3,  
CORFZN(6,60)=1.0e3,  
CORFZN(7,60)=1.0e3,  
CORFZN(8,60)=1.0e3,  
CORFZN(9,60)=1.0e3,

CORFRN(1,46)=1.0e3,  
CORFRN(2,46)=1.0e3,  
CORFRN(3,46)=1.0e3,  
CORFRN(4,46)=1.0e3,  
CORFRN(5,46)=1.0e3,  
CORFRN(6,46)=1.0e3,  
CORFRN(7,46)=1.0e3,  
CORFRN(8,46)=1.0e3,

CORFRN(1,47)=1.0e3,  
CORFRN(2,47)=1.0e3,  
CORFRN(3,47)=1.0e3,  
CORFRN(4,47)=1.0e3,  
CORFRN(5,47)=1.0e3,  
CORFRN(6,47)=1.0e3,  
CORFRN(7,47)=1.0e3,  
CORFRN(8,47)=1.0e3,

CORFRN(1,48)=1.0e3,  
CORFRN(2,48)=1.0e3,  
CORFRN(3,48)=1.0e3,  
CORFRN(4,48)=1.0e3,  
CORFRN(5,48)=1.0e3,  
CORFRN(6,48)=1.0e3,  
CORFRN(7,48)=1.0e3,  
CORFRN(8,48)=1.0e3,

CORFRN(1,49)=1.0e3,  
CORFRN(2,49)=1.0e3,  
CORFRN(3,49)=1.0e3,  
CORFRN(4,49)=1.0e3,  
CORFRN(5,49)=1.0e3,  
CORFRN(6,49)=1.0e3,  
CORFRN(7,49)=1.0e3,  
CORFRN(8,49)=1.0e3,

CORFRN(1,50)=1.0e3,  
CORFRN(2,50)=1.0e3,  
CORFRN(3,50)=1.0e3,  
CORFRN(4,50)=1.0e3,  
CORFRN(5,50)=1.0e3,  
CORFRN(6,50)=1.0e3,  
CORFRN(7,50)=1.0e3,  
CORFRN(8,50)=1.0e3,

CORFRN(1,51)=1.0e3,  
CORFRN(2,51)=1.0e3,  
CORFRN(3,51)=1.0e3,  
CORFRN(4,51)=1.0e3,  
CORFRN(5,51)=1.0e3,  
CORFRN(6,51)=1.0e3,  
CORFRN(7,51)=1.0e3,  
CORFRN(8,51)=1.0e3,

CORFRN(1,52)=1.0e3,  
CORFRN(2,52)=1.0e3,  
CORFRN(3,52)=1.0e3,  
CORFRN(4,52)=1.0e3,  
CORFRN(5,52)=1.0e3,  
CORFRN(6,52)=1.0e3,  
CORFRN(7,52)=1.0e3,  
CORFRN(8,52)=1.0e3,

CORFRN(1,53)=1.0e3,  
CORFRN(2,53)=1.0e3,  
CORFRN(3,53)=1.0e3,  
CORFRN(4,53)=1.0e3,  
CORFRN(5,53)=1.0e3,  
CORFRN(6,53)=1.0e3,  
CORFRN(7,53)=1.0e3,  
CORFRN(8,53)=1.0e3,

CORFRN(1,54)=1.0e3,  
CORFRN(2,54)=1.0e3,  
CORFRN(3,54)=1.0e3,  
CORFRN(4,54)=1.0e3,  
CORFRN(5,54)=1.0e3,  
CORFRN(6,54)=1.0e3,  
CORFRN(7,54)=1.0e3,  
CORFRN(8,54)=1.0e3,

CORFRN(1,55)=1.0e3,  
CORFRN(2,55)=1.0e3,  
CORFRN(3,55)=1.0e3,  
CORFRN(4,55)=1.0e3,  
CORFRN(5,55)=1.0e3,  
CORFRN(6,55)=1.0e3,  
CORFRN(7,55)=1.0e3,  
CORFRN(8,55)=1.0e3,

CORFRN(1,57)=1.0e3,  
CORFRN(2,57)=1.0e3,  
CORFRN(3,57)=1.0e3,  
CORFRN(4,57)=1.0e3,  
CORFRN(5,57)=1.0e3,

CORFRN(6,57)=1.0e3,  
CORFRN(7,57)=1.0e3,  
CORFRN(8,57)=1.0e3,

CORFRN(1,58)=1.0e3,  
CORFRN(2,58)=1.0e3,  
CORFRN(3,58)=1.0e3,  
CORFRN(4,58)=1.0e3,  
CORFRN(5,58)=1.0e3,  
CORFRN(6,58)=1.0e3,  
CORFRN(7,58)=1.0e3,  
CORFRN(8,58)=1.0e3,

CORFRN(1,59)=1.0e3,  
CORFRN(2,59)=1.0e3,  
CORFRN(3,59)=1.0e3,  
CORFRN(4,59)=1.0e3,  
CORFRN(5,59)=1.0e3,  
CORFRN(6,59)=1.0e3,  
CORFRN(7,59)=1.0e3,  
CORFRN(8,59)=1.0e3,

CORFRN(1,60)=1.0e3,  
CORFRN(2,60)=1.0e3,  
CORFRN(3,60)=1.0e3,  
CORFRN(4,60)=1.0e3,  
CORFRN(5,60)=1.0e3,  
CORFRN(6,60)=1.0e3,  
CORFRN(7,60)=1.0e3,  
CORFRN(8,60)=1.0e3,

CORFRN(1,61)=1.0e3,  
CORFRN(2,61)=1.0e3,  
CORFRN(3,61)=1.0e3,  
CORFRN(4,61)=1.0e3,  
CORFRN(5,61)=1.0e3,  
CORFRN(6,61)=1.0e3,  
CORFRN(7,61)=1.0e3,  
CORFRN(8,61)=1.0e3,

/

\*\*\*\*\*  
\*\*\*  
\*\*\* Output and plot variables  
\*\*\*  
\*\*\*\*\*

&XEDT

PRTC=100000,  
PPFC=100000,  
BSFC=100000,  
DMPC=100000,

DTPRT=100000.,  
DTPPF=100000.,  
DTBSF=2.0,0.2,1.0,2.0,5.0,  
DTDMP=100000.,

TCPRT=100000.,



TCPPF=100000.,  
TCBSF=200.,230.,300.,500.,1000.,  
TCDMP=100000.,

PCGRP(1)=50\*0,  
PPGRP(1)=50\*0,  
PRCEL(1,1)=250\*0,

SN(1)= 'ALPLK1', 'ALPLK2', 'ALPLK3', 'ALPLK4', 'ALPLK5', 'ALPLK6', 'ALPGK',  
SN(8)= 'PK', 'ALPSK1', 'ALPSK2', 'ALPSK3', 'ALPSK4', 'ALPSK5', 'ALPSK6',  
SN(15)= 'ALPSK7', 'ALPSK8', 'ALPSK9', 'TSK1', 'TSK2', 'TSK3', 'TSK4',  
SN(22)= 'TSK5', 'TSK6', 'TSK7', 'TSK8', 'TSK9', 'TLK1', 'TLK2',  
SN(29)= 'TLK3', 'TLK4', 'TLK5', 'TLK6', 'TGK', 'VK1', 'VK2',  
SN(36)= 'VK3', 'UK1', 'UK2', 'UK3', 'ALPINK', 'TIPINK',  
SN(42)= 'SIESK1', 'SIESK4', 'SIESK5', 'SIESK6', 'SIESK7', 'SIESK8', 'SIESK9',  
SN(49)= 'SIELK3', 'EIPINK', 'RBIK1', 'RBIK2', 'RBSK1', 'RBSK7', 'RBLK4',  
SN(56)= 'RBSK8', 'RBSK9', 'RBSK10', 'RBSK11',  
SN(60)= 'SVGK3', 'SVGK4', 'PGMK3', 'PGMK4', 'DHK',  
SN(65)= 'SVSK1', 'SVSK4', 'SVSK5', 'SVSK6', 'SVSK7', 'SVSK8',

/

\*\*\*\*\*  
\*\*\*  
\*\*\* Core power distribution (axial and radial profiles)  
\*\*\*  
\*\*\*\*\*

&XSOS

DAX(1)=23\*0.0,  
0.74,0.82,0.90,0.96,0.97,0.94,0.87,0.74,0.60,  
29\*0.0,  
DRAD(1)=0.94,0.96,0.99,1.02,1.04,1.18,1.10,0.0081,0.0081,  
18\*0.0,  
POW=1500.0D6,  
AMPTAB(1)=1.,1.,1.02,0.888,0.827,0.859,0.922,0.927,0.926,0.929,  
TIMAMP(1)=0.,200.,203.,210.,220.,243.,330.,400.,500.,700.,

/

\*\*\*\*\*  
\*\*\*  
\*\*\* Definition of regions and materials  
\*\*\*  
\*\*\*\*\*

&XERG

REGN=2  
REGC(1,1)=14,  
REGC(2,1)=1,  
REGC(3,1)=27,  
REGC(4,1)=61,  
REGC(1,2)=1,  
REGC(2,2)=1,  
REGC(3,2)=27,  
REGC(4,2)=61,  
MATEOS(2,1)=2,  
MATEOS(1,1)=2,  
MATEOS(5,2)=2,  
MATEOS(3,2)=3,

/